Investigation of the kynurenine metabolite profile of tryptophan degradation in the cuprizone toxin-induced demyelination animal model of multiple sclerosis

Helga Polyák M.Sc.

Ph.D. Thesis

University of Szeged
Albert Szent-Györgyi Medical School
Doctoral School of Clinical Medicine
Department of Neurology
Faculty of Medicine

Investigation of the kynurenine metabolite profile of tryptophan degradation in the cuprizone toxin-induced demyelination animal model of multiple sclerosis

Ph.D. Thesis

Helga Polyák M.Sc.

Supervisors: László Vécsei M.D., Ph.D., D.Sc.
Cecília Rajda M.D., Ph.D.

Szeged

2024

Original Publication directly related to the Ph.D. thesis:

I. **Polyák H.**, Cseh E.K., Bohár Zs., Rajda C., Zádori D., Klivényi P., Toldi J., Vécsei L. *Cuprizone markedly decreases kynurenic acid levels in the rodent brain tissue and plasma*. **Heliyon** 2021; 7:e06124. doi: 10.1016/j.heliyon.2021.e06124 (original paper**, IF: 3.776 (2021); Q1**)

II. **Polyák H.,** Galla Zs., Nánási N., Cseh E.K., Rajda C., Veres G., Spekker E., Szabó Á., Klivényi P., Tanaka M., Vécsei L. *The tryptophan-kynurenine metabolic system is suppressed in cuprizone-induced model of demyelination simulating progressive multiple sclerosis*. **Biomedicines** 2023, 11, 945. doi: 10.3390/biomedicines11030945 (original paper, **IF: 4.7 (2022); Q1**)

Cumulative impact factor of the publications directly related to the thesis: 8.476

Publications not directly related to the Ph.D. thesis:

I. Rajda C., Galla Zs., **Polyák H.**, Maróti Z., Babarczy K., Pukoli D., Vécsei L. *Cerebrospinal fluid neurofilament light chain is associated with kynurenine pathway metabolite changes in multiple sclerosis.* **Int. J. Mol. Sci. 2020**, 21, 2665. doi: 10.3390/ijms21082665 (original paper, **IF: 5.924 (2020); Q1)**

II. Cseh E.K., Veres G., Körtési T., **Polyák H.**, Nánási N., Tajti J., Párdutz Á., Klivényi P., Vécsei L., Zádori D. *Neurotransmitter and tryptophan metabolite concentration changes in the complete Freund's adjuvant model of orofacial pain*. **J. Headache Pain. 2020**, 21: 35. doi: 10.1186/s10194-020-01105-6 (original paper, **IF: 7.277 (2020); Q1)**

III. Pukoli D., **Polyák H.**, Rajda C., Vécsei L. *Kynurenines and neurofilament light chain in multiple sclerosis*. **Front. Neurosci. 2021**, 15: 658202. doi: 10.3389/fnins.2021.658202 **(IF: 5.152 (2021); Q2)**

IV. Tanaka M., Tóth F., **Polyák H.**, Szabó Á., Mándi Y., Vécsei L. *Immune influencers in action: metabolites and enzymes of the tryptophan-kynurenine metabolic pathway*. **Biomedicines 2021**, 9: 734. doi: 10.3390/biomedicines9070734 **(IF: 4.757 (2021); Q1)**

V. Tanaka M., Spekker E., Szabó Á., **Polyák H.**, Vécsei L. *Modelling the neurodevelopmental pathogenesis in neuropsychiatric disorders. Bioactive kynurenines and their analogues as neuroprotective agents—in celebration of 80th birthday of Professor Peter Riederer*, **J. Neural Transmi. 2022**, 129:627-642. doi: 10.1007/s00702-022-02513-5 **(IF: 3.3 (2022); Q3)**

VI. Tanaka M., Szabó Á., Spekker E., **Polyák H.**, Tóth F., Vécsei L. *Mitochondrial Impairment: A common motif in neuropsychiatric presentation? The link to the tryptophan–kynurenine metabolic system*. **Cells 2022,** 11: 2607. doi: 10.3390/cells11162607 **(IF: 6.0 (2022); Q2)**

Cumulative impact factor of publications not directly related to the thesis: 32.41

Total impact factor: 40.886

Posters directly related to the thesis:

I. **Polyák H.,** Galla Zs., Nánási N., Rajda C., Cseh E.K., Veres G., Klivényi P., Vécsei L. *A kinurenin útvonal részletes feltérképezése cuprizone rágcsáló modellben.* **Magyar Élettani Társaság Vándorgyűlése, MÉT - MMVBT 2022**; 2022. július 13-16.; Semmelweis Egyetem, Budapest, Magyarország

Posters not directly related to the thesis:

I. Rajda C., Csépány T., **Polyák H.**, Kiss A., Bencsik K., Szolnoki Z., Tóth L., Rózsa Cs., Semjén J., Bense E., Simon Zs., Dobos E., Tegze N., Jakab G., Katona G., Rácz Á., Eizler K., Rum G., Györök Gy., Lohner Zs., Füvesi J., Vécsei L. *Magyarországi több centrumos interferon-béta ellen termelődött kötődő ellenanyag vizsgálat – terápiás válasz az ellenanyag tükrében*, **III. MANIT, 2015, Budapest, Hungary**

II. Rajda C., Csépány T., Keresztes M., **Polyák H.**, Kiss A., Bencsik K., Szolnoki Z., Tóth L., Rózsa C., Semjén J., Bense E., Simon Z., Dobos E., Tegze N., Jakab G., Katona G., Lohner Zs., Füvesi J., Vécsei L. *Increased IFN-beta binding antibody levels in non-responding MS patients – a Hungarian multicentre study*, **ECTRIMS 2016, London, United Kingdom**

III. Rajda C., **Polyák H.**, Kelemen J., Dobner S., Liptai Z., Török T.K., Horváth R., Kuperczkó D., Bóné B., Bereg E., Vécsei L. *Tapasztalataink anti-MOG ellenanyag pozitív páciensekkel*, **IV. MANIT, 2017, Visegrád, Hungary.**

IV. Rajda C., Galla Zs., **Polyák H.**, Maróti Z., Babarczy K., Pukoli D., Vécsei L. *High neurofilament light chain and high quinolinic acid levels in the CSF of patients with multiple sclerosis are independent predictors of active, disabling disease,* **ECTRIMS 2019, Stockholm, Sweden**

V. Cseh E.K., Nikolett N., Veres G., **Polyák H.,** Körtési T., Vécsei L., Zádori D. *Development, validation and application of a HPLC method for the assessment of some tryptophan metabolites from murine samples*. In: Lukács, D.; Horváth, K.; Hajós, P. - Hungarian, Society for Separation Science (szerk.) Analysis of Carboxylic Acids with Ion Chromatography L36. **Pécs, Magyarország: Hungarian Society for Separation Sciences, (2019)** Paper: P-38

VI. Bíró Z., Kovács M., **Polyák H.**, Csépány T., Deme I., Illés Zs., Jakab G., Jobbágy Z., Lovas G., Mike A., Rózsa Cs., Simó M., Klivényi P., Rajda C. *Better symptomatic management and patient education are in the focus of interest of pwMS – an exploratory survey*. **8th EAN Congress 2022, Vienna, Austria**

VII. **Polyák H.,** Galla Zs., Rajda C., Klivényi P., Vécsei L. *Investigation of the kynurenine pathway in the cuprizone mouse model.* **11th Interdisciplinary Doctoral Conference; 25-26 November 2022, Pécs, 2022 Online**

VIII. **Polyák H.**, Galla Zs., Rajda C., Klivényi P., Vécsei L. *Investigation of the indole pathway of tryptophan metabolism in the cuprizone mouse model.* **International Neuroscience Conference, Pécs 2024; International Brain Research Organisation, Pécs 25-26 January, 2024, Hungary**

Table of contents

List of abbreviation

AMPA – amino-3-hydroxy-5-methyl-4-isoxazolepropionic

ANA – anthranilic acid

ATP – adenosine triphosphate

BBB – blood brain barrier

CIS – clinically isolated syndrome

CNS – central nervous system

CPZ – cuprizone

CO – control

DMT – disease-modifying therapies

DEM – demyelination

GFAP – glial fibrillary acidic protein

3-HANA – 3-hydroxyanthranilic acid

3-HK – 3-hydroxy-L-kynurenine

HPLC – high-performance liquid chromatography

IDO – indoleamine 2,3-dioxygenases

IHC – immunohistochemical

KAT – kynurenine aminotransferase

KMO – kynurenine 3-monooxygenase

KP – kynurenine pathway

KYN – kynurenine

KYNA – kynurenic acid

KYNU – kynureninase

LFB/CV – luxol fast blue - cresyl violet

MBP – myelin basic protein

MS – multiple sclerosis

NAD^+ – nicotinamide adenine dinucleotide

NEDA – no evidence of disease activity

NMDA – N-methyl-D-aspartate

PICA – picolinic acid

PIRA – progression independent of relapse activity

PMS – progressive multiple sclerosis

RAW – relapse-associated worsening

REM – remyelination

RNS – reactive nitrogen species

ROS – reactive oxygen species

RRMS – relapsing remitting multiple sclerosis

SPMS – secondary progressive multiple sclerosis

TDO – tryptophan 2,3-dioxygenase

TRP – tryptophan

UHPLCMS/MS – ultra-high performance liquid chromatography with tandem mass spectrometry

XA – xanthurenic acid

QUIN – quinolinic acid

Summary

Multiple sclerosis (MS) is an autoimmune, chronic inflammatory, demyelinating neurodegenerative disease of the central nervous system. The disease usually appears in young adulthood and is three times more common in woman. More than 2 million people worldwide suffer from MS. After years, with the progression of the disease, a permanent disability may gradually develop, which places a great burden on the patient, his narrower and wider environment. The root causes include genetic, lifestyle and environmental factors.

The cuprizone (CPZ) model is a toxin-induced demyelination rodent model of the MS, which is widely used to investigation the molecular factors that contribute to the demyelination and remyelination processes. The histopathological lesions induced by the CPZ toxin treatment are similar to the changes of type III MS lesion pattern. Despite intensive research on MS, its exact pathomechanims is still not fully understood, and further analysis is necessary. However, the described similarities make this animal model suitable and appropriate for studying the pathomechanims of MS.

A significant part of the breakdown of the essential amino acid tryptophan takes place via the kynurenine pathway (KP), and the serotonin pathway. During the degradation, various neuroactive metabolites are produced, which have a notable biological role in different physiological processes. The role of the KP in neurological pathologies has become increasingly well-known, as differences in the concentration levels of some metabolites in the pathway have been detected in various neurodegenerative diseases, including MS.

We used the CPZ toxin-induced demyelination rodent model, which represents the progressive form of the MS, to investigate the differences in the concentrations of the metabolites produced in tryptophan breakdown, at different times of the CPZ treatment and recovery period, thereby completely mapping the KP.

During our investigation, we experienced significant decrease in the levels of various KP metabolites, including anthranilic acid, 3-hydroxy-L-kynurenine, kynurenic acid and xanthurenic acid, as well as a notable increase in the concentration of tryptophan during the toxin treatment, in the periphery and central nervous system, which differences disappeared in the recovery period. Our results allow us to conclude that CPZ treatment can affect certain metabolites of tryptophan degradation in demyelination and remyelination processes.

Introduction

Multiple sclerosis

Multiple sclerosis (MS) is one of the most common non-traumatic, immune-mediated, chronic inflammatory, demyelinating, multifocal and progressive disease of the central nervous system (CNS) [1,2], which can be characterized by the lesions caused by demyelination, loss of axons and oligodendrocytes, gliosis, axonal damage, and loss of neurons in the brain and spinal cord [3–8]. Worldwide, approximately 2.8 million people suffer from this disease [9]. MS usually appears in young adulthood, placing a heavy burden on those affected by the disease, society and the economy [10,11]. The MS can be typified by gender differences, which is affecting the severity and occurrence of the disease [12]. In the case of men, generally the disease has a worse course, with a rapid accumulation and progression of disability, but the appearance of the disease is much more common among woman [12–14]. The specific root cause of the disease is not yet completely clear however, various environmental, genetic and epigenetic factors may contribute to the development of the MS, for example Epstein-Barr virus infection, exposure to ultraviolet B radiation, vitamin D status, smoking, obesity in childhood, and the individual genetic background contributes to all of this [2,12,15,16].

The exact pathomechanism of the disease, as well as the various molecular and metabolic processes behind the neuro-axonal damage are not completely clear, however oxidative stress largely contributes to the progression of MS, causing neuronal and axonal injury [17,18]. Furthermore, the malfunctioning and regulation of the immune system, the disturbances in the balance of pro- and anti-inflammatory cytokines, the disruption of the blood-brain barrier, and the activation of glial cells are also important influencing factors [19–23]. CNS infiltration of peripheral T and B immune cells, and macrophages, as well as the CNS reactivity of astrocytes and microglia, cause excessive production of inflammatory cytokines and reactive oxygen species (ROS), which ultimately results in oxidative stress in addition to reduced antioxidant activity [22,24]. Based on research, in addition to oxidative stress and inflammatory responses mediated by the immune system, other neurodegenerative processes, including glutamate excitotoxicity and mitochondrial dysfunction also contribute to the pathogenesis and progression of MS [18].

In some cases, MS begins with as a clinically isolated syndrome (CIS) involving one or more CNS regions on the MRI including an acute-subacute clinical event. In some cases, the CNS inflammation allows the immediate diagnosis of relapsing remitting (RR) MS. The CIS can

transform into a RR form (RRMS). In this form of the disease is characterized by worsening and improving phases, i.e. every clinical event is usually followed by recovery form it [25–27]. Furthermore, in RRMS, demyelination, T and B cell inflammatory reactions, microglial activation, mitochondrial damage, its dysfunction and lack of energy; as well as oxidative damage can be observed, which ultimately leads to the formation of plaque [28,29]. However, recovery from relapses is not complete; and disability accumulates over time, and years later, the RRMS form of the disease transforms into a secondary progressive multiple sclerosis (SPMS) in a significant number of patients [25,27,30,31]. When additional atrophy and axon damage occur in the white and gray matter, probably with neurodegenerative processes, but less inflammation [25,29,32]. Nevertheless, to a lesser extent, MS can also begin with the progressive form of the disease (PPMS) [25,27,33], which can be characterized by spinal cord dysfunction, further microglial activation with atrophy, more diffuse axon loss of the brain, and neurodegeneration with energy deficit and oxidative damage [25,28,29]. However, disability can accumulate irreversibly at any stage of the disease through two main mechanisms, the progression independent of relapse activity (PIRA) and relapse-associated worsening (RAW) [34,35]. PIRA is mainly related to an underlying neurodegenerative component and can be considered one of the most important mechanisms in MS [34–38]. If PIRA is the leading event in the disease course, it is considered to be the most unfavorable prognostic sign [35]. For this reason, appropriate treatment of the disease is extremely important. Current treatments concentrate on reducing disease activity, treating attack and alleviating symptoms with disease modifying therapies (DMT) [39]. DMT influence the course of MS by suppressing or modulating the functions of the immune system, thereby preventing or delaying long-term disability [2,39]. Treatments of the MS can be immunomodulatory (as interferon-beta, glatiramer acetate, teriflunomide), and immunosuppressant (such as fingolimod, natalizumab), during which continuous therapy is required to permanently suppress disease activity and inflammation. However, there are immune reconstitution therapies (for example cladribine, alemtuzumab), which are short-term treatments to achieve lasting immunological effects [39]. Recently, the NEDA point of view, i.e. “no evidence of disease activity” has become widespread in the MS therapy, which means that the patient is not showing symptoms of radiological and clinical activity. Radiological activity is characterized by new or enlarging T2 lesions or new Gd enhancing lesions, until clinical activity is characterized by releases or confirmed disease progression by 3 or 6 month. Brain atrophy is difficult to detect and can progress even without obvious inflammatory disease activity, and continuous inflammatory MRI activity that exceeds clinical relapses. In

cases of high clinical activity, more specialized, highly efficacious treatments are justified in the first instance [2]. Furthermore, symptomatic treatments include pharmaceutical and physical therapies too, that target symptoms resulting from damage of the CNS, as fatigue, cognitive impairment, neuropathic pain, bladder dysfunction and spasticity. These treatments usually are not MS specific, however, they are extremely crucial for patients with MS in the treatment of disabling symptoms [2,25].

Cuprizone model, as the multiple sclerosis rodent model

For the investigation of the MS pathomechanism, there are several animal model, among others bis(cyclohexanone)oxaldihydrazone (cuprizone, CPZ) toxin-induced demyelination model. The CPZ model is excellent for examining molecular factors and pathological changes that contribute to demyelination and remyelination processes, in the lack of peripheral immune response, and without disruption of the BBB [21,40–42]. Copper (Cu^{2+}), is a cofactor of many copper enzymes and plays an important role in various cellular processes, therefore any disturbance in its homeostasis can result in neurodegeneration [21]. The CPZ toxin is a copper chelating agent that selectively induces apoptosis of mature oligodendrocytes [41,43], which toxicity can results from disrupting the very active metabolism of oligodendrocytes [21]. CPZ affects the function of the mitochondrial respiratory chain by inhibiting certain mitochondrial complexes [21]. Furthermore, megamitochondrial formations were recorded during intoxication in oligodendrocytes and liver, but no signs of poisoning were observed, among others neurons, microglia, astrocytes or heart cells or oligodendrocyte precursor cells, only in mature oligodendrocytes (for a detailed review, see [21]). This megamitochondrium formation is the consequence of the effect of increased ROS and reactive nitrogen species (RNS), it can be considered a defense mechanism of the cell, by which it tries to reduce oxidative stress [44]. The lack of adenosine triphosphate (ATP) and increased concentration of ROS/RNS, caused by megamitochondrium formation disrupts the normal endoplasmic reticulum function, this damages protein and lipid synthesis, which results in the degeneration of the oligodendrocyte perikaryon and finally the disintegration of the myelin sheath [21]. However, poisoning-induced mature oligodendrocyte cell death is not evenly distributed in the CNS, with extensive demyelination observed in the corpus callosum, cortex, striatum, hippocampus and cerebellum, as well as to a limit extent in the brainstem and spinal cord [40]. CPZ can also induce axonal damage in white and gray matter regions, which damage can cause loss of synaptic connections and thus lead to functional deficits and prolonged disability (for a review, see [40]). Furthermore, CPZ provokes glutamate excitotoxicity/synaptotoxicity

through its effect on the expression of glutamate receptor subunits in corpus callosum, cortex, or hippocampal neurons [40,45,46].

In the first few weeks of CPZ treatment, oligodendrocytosis begins, followed by microglia, macrophage and astrocyte activation. In addition, demyelination can also be observed, which damage becomes more severe in the 4-5 weeks of the treatment, this is the “acute phase” of the treatment [40,47,48]. The increased glia activity enables the removal of myelin debris produced during the damage, but this glial reactivity further aggravates oligodendrocytosis and the demyelination process [40,47,49,50]. However, if the CPZ treatment is discontinued, rapid regeneration occurs, when mature oligodendrocytes are formed from the oligodendrocyte progenitor cells during remyelination and the gliosis gradually ceases [21,40,47,48,51]. Chronic CPZ treatment exceeding 12 weeks results in extensive gliosis, severe demyelination, reduced body weight of animals and higher mortality, and the efficiency of the remyelination is also significantly limited; this chronic phase already models the later stages of the MS disease [40,52,53].

The CPZ toxin-induced demyelination rodent model is highly relevant in the study of the pathomechanism of MS, since this model represents the progressive phase of the disease. In MS 4 different lesion subtypes have been described [54]. Types I and II are believed to be autoimmune-mediated, defined by limited oligodendrocyte dystrophy and the involvement of immunoglobulin G/complement complexes, while lesion pattern III and IV are characterized by primary oligodendrogliopathy with depletion and apoptosis of mature oligodendrocytes and the relatively intact BBB. However, the common feature of all 4 subtypes is infiltration of macrophages and T-lymphocytes, as well as myelin oligodendrocyte glycoprotein (MOG), proteolipid protein (PLP), myelin basic protein (MBP), or myelin associated glycoprotein (MAG) reduction [21,40,54–56]. The type III lesion pattern shows several similarities with the lesions caused by the CPZ toxin, including active demyelinating lesions presence of few T cells, but a significant involvement of microglia and macrophages, or hypoxia-like tissue damage with metabolic stress and mitochondrial deficit, which cause oligodendrocyte apoptosis [21]. During CPZ poisoning, the BBB remains unaffected, which limits the infiltration of T and B cells, i.e. peripheral immune cells, into the CNS. Thus, the CPZ model can be suitable for the examination and full exploration the underlying mechanisms involved in the progressive stages of MS, which processes are independent of the infiltration of adaptive immune cells into the CNS [40,57]. These similarities during the demyelination process, as well as the joint study of the remyelination phase, which can be easily influenced by the length

of the CPZ toxin treatment, make the CPZ model advantageous and relevant in the investigation of the pathomechanims of MS.

Tryptophan metabolism

The essential amino acid tryptophan (TRP) is metabolized to a significant extent, approximately 95%, though the kynurenine pathway (KP), which takes place in astrocytes, neurons, microglia, and macrophage cells; and a lesser extent via the serotonin pathway [58–61] **(Figure 1.)**. The metabolism of TRP can be associated with the functioning of the nervous system, inflammation and immune system processes [62]. The serotonin pathway produces, among others 5-hydroxy tryptophan, serotonin or melatonin. Serotonin, as a neurotransmitter, participates in the regulation of neuroendocrine functions, and plays an important role in inflammatory diseases of the CNS, including MS [62,63]. However, the vast majority of TRP is degraded by the KP, the first step of which is the conversion of TRP to l-kynurenine (KYN) catalyzed by indoleamine 2,3-dioxygenases (IDOs) and TRP 2,3-dioxygenase (TDO) enzymes. Subsequently, in three branches different metabolite are formed from KYN, such as kynurenic acid (KYNA) by kynurenine aminotransferases (KATs), kynureninase (KYNU) enzyme catalyzed the conversion of KYN to anthranilic acid (ANA), and kynurenine 3-monooxygenase (KMO) is responsible for the formation of 3-hydroxy-L-kynurenine (3-HK). Furthermore, on the one hand, xanthurenic acid (XA) can be formed from 3-HK. On the other hand, 3-HK can be degrade to 3-hydroxyanthranilic acid (3-HANA), from which among others picolinic acid (PICA), quinolinic acid (QUIN) are formed and finally nicotinamide adenine dinucleotide (NAD+) is produced at the end of the KP [58,62] **(Figure 1.)**.

Various neuroactive metabolites are formed during TRP degradation, such as KYNA and PICA, which are thought to be neuroprotective; and the QUIN and 3-HANA, which are considered neurotoxic [64,65]. KYNA influences glutamatergic neurotransmission on glutamatergic receptor subunits, it is a competitive antagonist on N-methyl-D-aspartate (NMDA) receptors, and has a weak antagonistic effect on amino-3-hydroxy-5-methyl-4-isoxazolepropionic (AMPA) and kainate receptors [66–68]. In addition, it indicates a significant immunomodulating role, that KYNA is also a strong aryl hydrocarbon-receptor ligand [69]. Furthermore, KYNA is thought to be protective at certain concentrations by scavenging ROS [58,69]. Nevertheless, QUIN is a competitive NMDA receptor agonist, which can induce glutamatergic excitotoxicity, thereby causing neuronal cell death [64,70,71].

In the KP, several abnormalities have been observed in various neurodegenerative disorders, including MS [58,64,68,72,73]. In the progressive form of the disease, there was a decreased in KYNA level, while in relapsing MS the pathway has shifted towards QUIN [74,75]. Furthermore, increased QUIN and decreased KYNA and PICA concentration were observed in the cerebrospinal fluid of MS patients [58]. In addition, the KYNA level increased during relapse, while it decreased in the remission phase. Recently, a decreased in the 3-HK concentration was reported in the serum of MS patients [76].

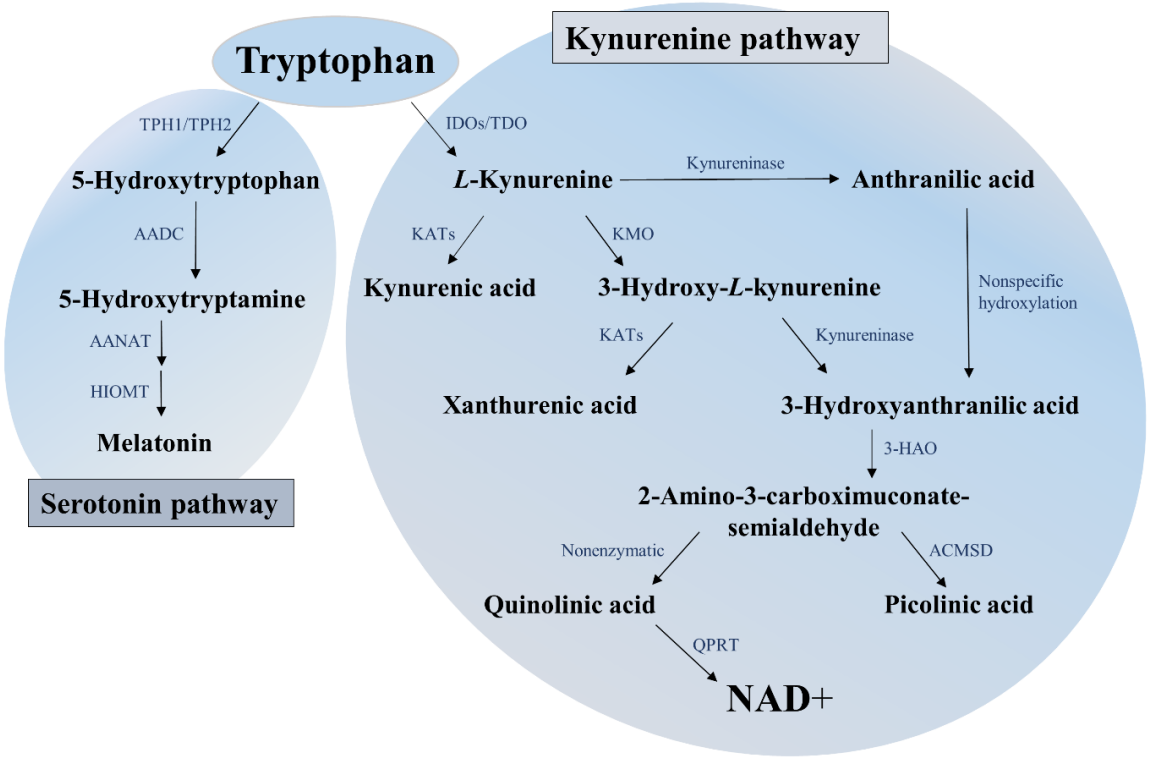

Figure 1. The serotonin and kynurenine pathway of tryptophan breakdown. 3-HAO: 3-hydroxyanthranilate oxidase; AADC: aromatic-L-amino-acid decarboxylase; AANAT: aryl alkylamine N-acetyltransferase; ACMSD: α-amino-carboxymuconate-semialdehyde-decarboxylase; HIOMT: hydroxyindole-O-methyltransferase; IDOs: indoleamine 2,3-dioxygenases; TDO: tryptophan 2,3-dioxygenase; KATs: kynurenine aminotransferases; KMO: kynurenine 3-monooxygenase; NAD^+: nicotinamide adenine dinucleotide; TPH1/TPH2: tryptophan 5-hydroxylase; QPRT: quinolinate phosphoribosyltransferase.

Aims

I. After the successful establishment of the CPZ toxin-induced MS rodent model, our plans included the examination of the concentration of TRP, 5-HT, L-KYN and KYNA metabolites in the serotonin and kynurenine pathways of TRP metabolism, as we hypothesized that in MS detected KP shifts and deviates, such as reduced levels of TRP and KYNA, as well as an increased KYN concentration can also be found in the CPZ model.

II. Based on our previous results, the further goal of our examination was the detailed mapping of the metabolites involved in the kynurenine pathway of the TRP degradation during the CPZ toxin treatment and recovery phase. We assumed that, in addition to KYNA, other neuroactive metabolites in the KP may also show differences as a result of CPZ. Presumably, the concentration of some neurotoxic metabolites, for example QUIN and 3-HANA increases, while the levels of XA and ANA, which are believed to be neuroprotective, decrease.

Materials and methods

Animals

In our investigations, eight-week old male C57Bl/6J mice were used (*n* = 224). The animals were bred and maintained under standard laboratory conditions with 12 h–12 h light/dark cycle at 24 ± 1 ºC and 45–55% relative humidity in the Animal House of the Department of Neurology, University of Szeged. The investigations were in accordance with the Ethical Codex of Animal Experiments and were approved by the Ethics Committee of the Faculty of Medicine, University of Szeged, and the National Food Chain Safety Office with a permission number of XI/1101/2018. The animals were housed in polycarbonate cages (530 cm^3 floor space) in groups of 4-5. Prior to the start of the experiments, all animals were acclimated to grounded standard rodent chow for 2 weeks, and animal's weight was measured every other day, thus monitoring the health status of the mice during acclimatization. Furthermore, during the entire duration of our experiments, in both the CPZ treatment (demyelination) and the recovery (remyelination) phase, we measured the animal's body weight every other day.

I. Analysis of TRP metabolism following the setting of the CPZ toxin-induced demyelination rodent model

Treatment

In our investigations, during the setting of the CPZ model [22], half of the experimental animals (*n* = 52), as the CPZ group, were given a diet containing 0.2% CPZ toxin (bis-cyclohexanone-oxaldihydrazone; Sigma-Aldrich) for 5 weeks mixed into a grounded standard rodent chow with free access to water. For control group (CO), age and weight-matched animals were used, which had rodent chow and free access to water. At the end of 5-week CPZ treatment (demyelination period), half of the animals in the CPZ treated (*n* = 36) and control (*n* = 28) groups were randomly chosen and sacrificed. The surviving animals (CPZ *n* = 18; CO *n* = 14) participated in a 4-week recovery phase (remyelination period). At the end of 4^{th} week, the remaining animals were sacrificed too, sample collection purpose. During the examination, at the end of demyelination and remyelination phase, behavioral tests were performed **(Figure 2.)** [22].

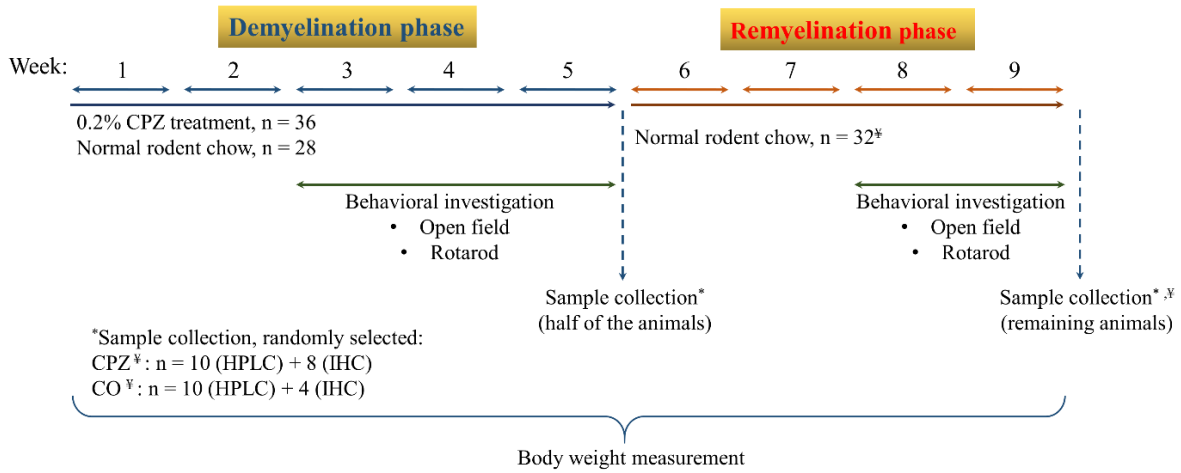

Figure 2. Timeline of the experimental procedure used [22]. CPZ: cuprizone; CO: control; IHC: immunohistochemical studies; HPLC: High-performance liquid chromatography; n: the number of animals. ¥One animal died in cage at the beginning of the remyelination phase in the CPZ treated group and at the end of the remyelination phase, an animal also died in the CO group before perfusion. *Sample collection was randomly selected in the CPZ treated- and the CO group.

Prior the perfusion, animals were anesthetized with intraperitoneal 4% chloral hydrate (10 ml/kg body weight). The mice were perfused transcardially with artificial cerebrospinal fluid followed by 4% paraformaldehyde in 0.1 M phosphate buffer for the histological and immunohistochemical (IHC) studies (CPZ: *n* = 16, CO: *n* = 8). Brain samples were dissected and postfixed in the 4% paraformaldehyde overnight at 4ºC. Brains were embedded in paraffin, coronally sectioned in 8 µm thickness obtained from different regions (0.14, -0.22, -1.06, and -1.94 mm) according to the mouse brain atlas of Paxinos and Franklin (2001) and placed on gelatin-coated slides [77]. For bioanalytical measurements, the animals (CPZ: *n* = 20, CO: *n* = 20) were anesthetized and perfused as described above. Blood samples were taken from the left heart ventricle into Eppendorf tubes containing 5% disodium ethylenediaminetetraacetate dihydrate (EDTA) and the plasma was separated by centrifugation (3500 rpm for 10 min at 4 ºC). The brains were dissected into five different brain regions, including the cerebellum, brainstem, striatum, somatosensory cortex and hippocampus. All samples were removed on ice and stored at -80 ºC until further use. The CPZ treated and recovered mice were marked as groups demyelination (DEM) and remyelination (REM), respectively, whereas age matched animals, as controls became the CO1- and CO2 group.

Behavioral tests

The testing procedures were performed during the light phase (between 8 a.m. and 12 p.m.) in a quiet room, after 1 hour of habituation. During the investigation, we performed the open field test, each animal (n = 18/group) in CPZ treated and CO groups was placed in the center of an open-field box measuring 48 * 48 * 40 cm for 15 min tracking periods (analyzed in three 5 min periods). The movement patterns of the animals were tracked and recorded with the Conducta 1.0 system (Experimetria Ltd.). The parameters recorded were the ambulation distance, the time spent in immobility and the total time spent with consecutive rearing [78]. Open field measurements were carried out in the 3rd, 4th and 5th week of CPZ poisoning and in the 3rd and 4th week of the remyelination phase, once a week on the same day.

To determine the effects of CPZ treatment on motor function we applied the rotarod test. The animals in the CPZ and CO groups (n = 18/group) were trained on the rotarod for a 3-session period for 5 min on 2 consecutive days prior to the first test day. On the first and second days of the training sessions, a constant speed of 5 and 10 rpm respectively, was used. The investigation was performed on the 3rd, 4th and 5th week of CPZ intoxication and on the 3rd and 4th week of the recovery phase, once a week on the same day following the training sessions. The performance of each mouse was measured three times with resting periods of 30 min between consecutive tracking sessions. The latencies to fall values were recorded with the TSE Rotarod Advanced system. In the test phase, rodents were placed on a rotating rod, with a constantly increasing speed from 5 to 40 rpm during the 300 min test period. On the day before the respective test day, a 3 session retraining at 10 rpm for 5 min with 30 min resting periods was carried out to enable the animals to recall the rotarod experience [78].

Immunohistochemistry and intensity measurement analysis

For immunohistochemical analysis gelatin-coated slides were deparaffinized, rehydrated and heat-unmasked in 10 mM citrate buffer. Sections were blocked with 0.3% hydrogen peroxide in phosphate-buffered saline (PBS) solution and incubated with the primary antibody diluted in a solution containing 0.1 M PBS and 10% normal goat or horse serum overnight. Anti-glial fibrillary acidic protein (GFAP, 1:500, rabbit IgG, Dako, Agilent) for astrocyte visualization and anti-myelin basic protein (MBP, 1:500, mouse IgG, Abcam) to detect myelin were applied. Adequate biotinylated secondary antibody was used and the ABC Kit (Vectastain Kit, Vector Laboratories) and 3,3'-diaminobenzidine (DAB) reaction was used for visualization. For measurements an AxioImager M2 microscope, equipped with an AxioCam MRc was applied. Rev 3 camera (Carl Zeiss Microscopy) and AxioVision 4.8 software (Carl Zeiss

Microscopy, Germany) program were used. Quantification of astrogliosis was performed by manual cell counting of the GFAP-immunopositive cells in the corpus callosum. Intensity measurement was applied to determine myelin content with MBP staining.

Myelin damage was evaluated with luxol fast blue - cresyl violet (LFB/CV) staining. The brain slides were deparaffinized, rehydrated with 95% alcohol and incubated in a 0.01% LFB solution overnight at 60 ºC, after that the sections were differentiated in 0.05% lithium carbonate solution and counterstained with CV. The myelin content was determined by intensity measurement after LFB staining.

High-performance liquid chromatography (HPLC) measurement

Chromatographic separation was carried out with a validated method, as described before [79]. Briefly, on the day of measurement, plasma and brain samples were deproteinized by precipitation, as described before [79]. The mobile phase, in each case was a 200 mM zinc acetate solution, at final pH of 6.2 for plasma, and 5.8 for brain tissue samples, with a final concentration of 5 % of acetonitrile. Regarding the LOD values, in brain samples it was 0.259 nmol/g ww for KYN and 1.82 for KYNA, whereas in plasma samples it was 1.33 nM for KYNA.

Statistical analysis

For the quantitative evaluation of GFAP-immunopositive cells and the analysis of intensity measurement of LFB and MBP statistical differences were determined by one-way analysis of variance (ANOVA) followed by the Sidak or Tamhane's T2 post hoc test depending on variances of data, with $p < 0.05$ taken as statistically significant. For statistical comparison of the body weight and behavioral measurements, we used two-way repeated measures ANOVA. Pairwise comparisons of group means were based on the estimated marginal means with Sidak or Tamhane's T2 post hoc test with adjustment for multiple comparisons. Group values are described as means ± SEM, analyses were performed in SPSS Statistics software (version 20.0 for Windows, SPSS Inc). Regarding the HPLC measurements, if the distribution (Shapiro–Wilk test) was proven to be Gaussian and the variances were equal (Levene test) ANOVA was used with Tukey HSD post hoc test for pairwise comparison, otherwise Kruskal-Wallis, with the Wilcoxon post hoc test was applied. Data were plotted as median (1st–3rd quartile).

II. Mapping of metabolites concentration involved in the kynurenine pathway TRP metabolism in the CPZ-induced rodent model

Treatment

Similar to our previous study, half of the experimental animals (*n* = 80) were administered 0.2% CPZ toxin (bis-cyclohexanone-oxaldihydrazone; Sigma-Aldrich) for 5 weeks with food containing, mixed into a grounded standard rodent chow with free access to water. The age and weight-matched control (CO) animals (*n* = 80) were fed normal rodent chow and had free access to water. At the end of the 1st, 3rd, and 5th weeks, 16 animals were randomly chosen from both CO and CPZ groups and terminated for further analysis. Thus, at the end of the demyelination phase, 96 animals were terminated (*n* = 96, 48 CPZ-treated, and 48 control animals). The surviving animals (*n* = 64, 32 CPZ treated, and 32 control animals) underwent the recovery period for 4 weeks and at the end of the 2nd and 4th weeks of the remyelination phase they were sacrificed **(Figure 3)**. The animals were terminated according to our previous investigation [22]. The mice were anesthetized with intraperitoneal 4% chloral hydrate (10 mL/kg body weight). For the histological and immunohistochemical studies, mice (CPZ: *n* = 30, CO: *n* = 30) were perfused transcardially with artificial cerebrospinal fluid followed by 4% paraformaldehyde in 0.1 M phosphate buffer. Brain samples were dissected and postfixed in the same fixative overnight at 4 ºC. Brains were embedded in paraffin, coronally sectioned in 8 µm thickness obtained from four diverse regions (0.14, -0.22, -1.06, and -1.94 mm) according to the mouse brain atlas of Paxinos and Franklin (2001) and placed on gelatin-coated slides [77]. For bioanalytical measurements, the animals (CPZ: *n* = 50, CO: *n* = 50) were anesthetized and perfused as described above. Blood samples were taken from the left heart ventricle into Eppendorf tubes containing 5% EDTA and plasma was separated by centrifugation (3500 rpm for 10 min at 4 ºC). The brains were dissected into five distinct brain regions, including the cerebellum, brainstem, striatum, somatosensory cortex, and hippocampus. All samples were placed on ice and stored at -80 ºC. The samples were marked as groups of DEM, REM, or CO.

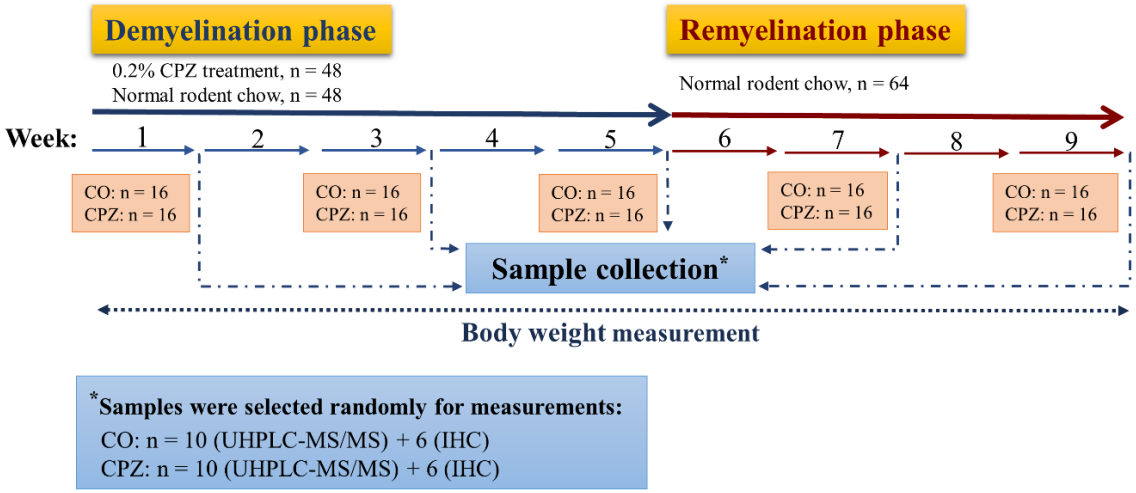

Figure 3. Timeline of the experimental procedure applied in this study [41]. CO: control group; CPZ: cuprizone group; IHC immunohistochemical studies; n the number of animals; UHPLC-MS/MS: Ultra-high performance liquid chromatography with tandem mass spectrometry; *: random sample selection

Histological analyses and myelin content determination

Myelin damage was estimated by LFB/CV staining, using with same protocol, as for the CPZ mouse model setup. Briefly, the brain slides were deparaffinized, rehydrated with 95% alcohol, incubated in a 0.01% luxol fast blue solution overnight at 60 ºC, after that the sections were differentiated in 0.05% lithium carbonate solution and counterstained with CV. For measurements of the stained sections were taken using a Zeiss AxioImager M2 microscope, supplied with an AxioCam MRc Rev. 3 camera (Carl Zeiss Microscopy). Zeiss Zen 2.6 (blue edition)® image analysis software program was used. LFB/CV staining was performed to determine the degree of myelin damage, then the corpus callosum was marked on each section based on the mouse brain atlas, and intensity measurement was applied on this designated area in order to determine myelin content.

Ultra-High-Performance Liquid Chromatography with Tandem Mass Spectrometry Measurement

All reagents and chemicals were of analytical or liquid chromatography–mass spectrometry grade. TRP and its metabolites, and their deuterated forms: d4-SERO, d5-TRP, d4-KYN, d KYNA, d4-XA, d5-5-HIAA, d3-3-HANA, d4-PICA, and d3-QUIN were obtained from Toronto Research Chemicals (Toronto, ON, Canada). d3-3-HK was obtained from Buchem B. V. (Apeldoorn, The Netherlands). Acetonitrile (ACN) was provided by Molar Chemicals

(Halásztelek, Hungary). Formic acid (FA) and water were purchased from VWR Chemicals (Monroeville, PA, USA). Methanol (MeOH) was acquired from LGC Standards (Wesel, Germany). The preparation of the standards, internal standards (IS), as well as quality control (QC) solutions were necessary for the measurement, and the preparation of the plasma sample of animals for analysis, which was based on the description published by Tömösi et al. [80]. The brain samples, after measuring the weight of the five different brain regions, we homogenized them (UP100H, Hielscher Ultrasound Technology, Germany; amplitude: 100%, cycle: 0.5) in 3x amount of ice-cooled LC-MS water (for example, 90 µL water was pipetted to 30.0 mg sample). After that, the same steps as for the plasma samples were performed, with the difference that the precipitation was carried out with 100% acetonitrile. Then, plasma samples and brain regions were measured according to the previously published methodology using UHPLC-MS/MS [81]. Multiple reaction monitoring (MRM) transition of PICA was 124.0/106.0 using 75 V as declustering potential and 13 V as collision energy, retention time: 1.21 min.

Statistical Analysis

For the statistical analysis of body weight, two-way repeated-measures ANOVA was applied. For the densitometric analysis of LFB/CV statistical differences were determined by one-way analysis of variance (ANOVA), then depending on the variances of data, Sidak or Tamhane's T2 post hoc test was used. Pairwise comparisons of group means were based on the estimated marginal means with Sidak or Tamhane's T2 post hoc test with adjustment for multiple comparisons. Group values were given as means ± SEM, analyses were performed in SPSS Statistics software (version 20.0 for Windows, SPSS Inc. IBM, Armork, NY, USA). Regarding the UHPLC-MS/MS measurements, all statistical analyses were performed with the help of the R software (R Development Core Team). After checking for its assumptions (checking for outliers, Shapiro and Levene tests), we performed two-way ANOVA with estimated marginal means post hoc tests to determine significance between treatment groups, measurement times, and their interaction. In case of the assumptions were not met, we used the Sheirer–Ray–Hare test with Dunn test as post hoc. Type I errors from multiple comparisons were controlled with the Bonferroni method. We rejected null hypotheses when the corrected p level was < 0.05, and in such cases, the differences were considered significant.

Results

I. Analysis of TRP metabolism following the setting of the CPZ toxin-induced demyelination rodent model

Body weight measurement

During our investigation, already on the third day of the CPZ treatment, a significant decrease was detected in the body weight of the CPZ treated group compared to the CO group **(Figure 4)**. This difference remained until the end of the demyelination phase. However, this disparity disappeared in the first few days of the recovery phase and the body weight of the two groups was in the same range by the end of the experiment.

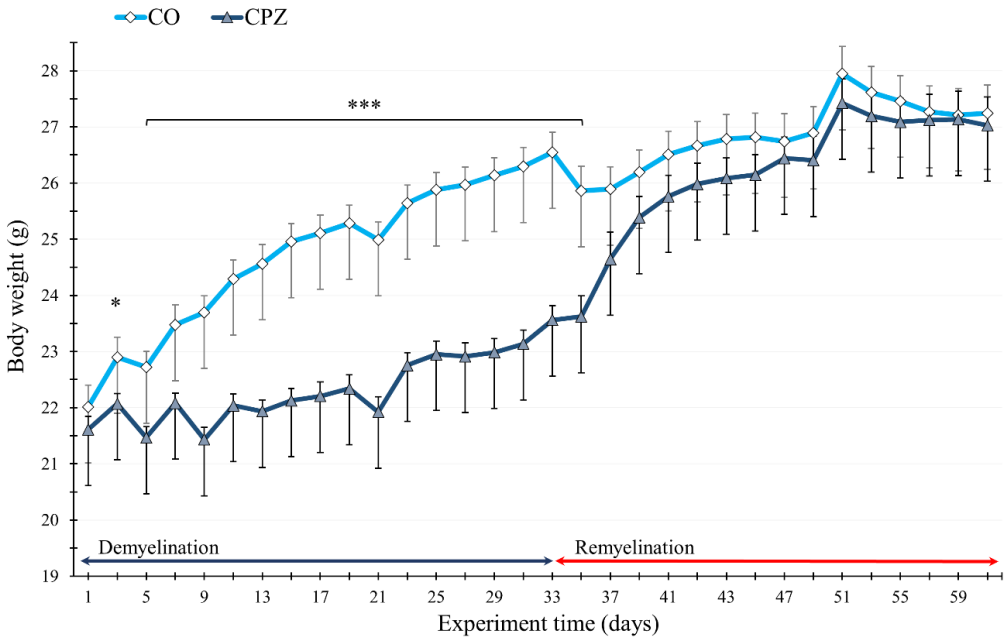

Figure 4. Differences in body weight of animals during investigation. The CO group is depicted with white diamonds and CPZ toxin treated group is depicted with gray triangles. The demyelination and remyelination period are indicated with blue and red arrows, as the two major parts of the experiment. CO: control group; CPZ: cuprizone treated group, *: $p < 0.05$ vs. CO, ***: $p < 0.001$ vs. CO. The data are presented as mean ± SEM.

Determination of damage caused by cuprizone toxin treatment

The 5-week CPZ treatment caused an extensive myelin damage within the corpus callosum at the end of the demyelination period, which is illustrated by the MBP **(Figure 5)** and LFB/CV staining **(Figure 6, Figure 8B-C)**. However, the degree of demyelination decreased by the 4th

week of the recovery phase. Furthermore, the GFAP immunostaining **(Figure 7)** showed a significant astrogliosis in the area of corpus callosum in CPZ-treated animals compared to the control group, both in the demyelination and remyelination phases **(Figure 8A)**.

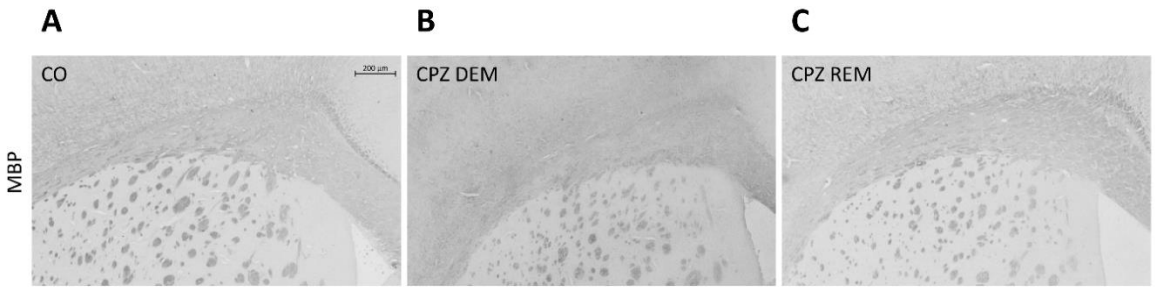

Figure 5. Determination of myelin content by MBP staining in the CO (A), CPZ DEM (B) and CPZ REM (C) group. In the CPZ-treated group (B), a reduced myelin content was observed, which increased in the remyelination phase (C). Scale bar: 200 µm. CO: control group, CPZ: cuprizone treated group, DEM: demyelination phase of the CPZ-treated group, MBP: myelin basic protein, REM: remyelination phase of the CPZ-treated group.

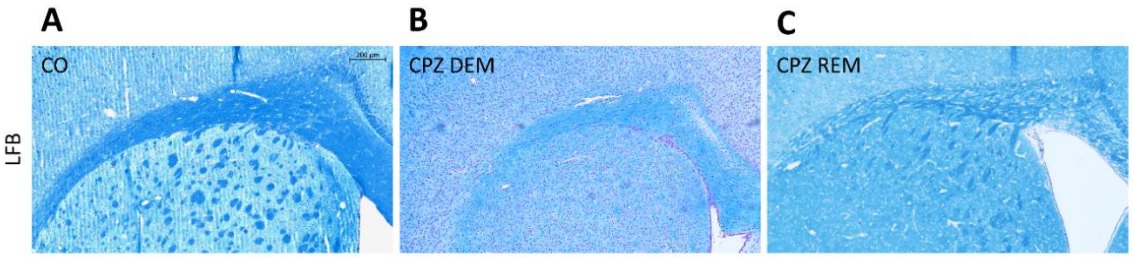

Figure 6. LFB/CV staining in the corpus callosum of the CO (A), CPZ DEM (B) CPZ REM (C) group. The CPZ-treated group (B) showed a decreased myelin content compared to the CO group (A), which elevated during the remyelination phase (C). Scale bar: 200 µm. CO: control group, CPZ: cuprizone treated group, DEM: demyelination phase in the treated group, LFB/CV: luxol fast blue - cresyl violet, REM: remyelination phase in the treated group.

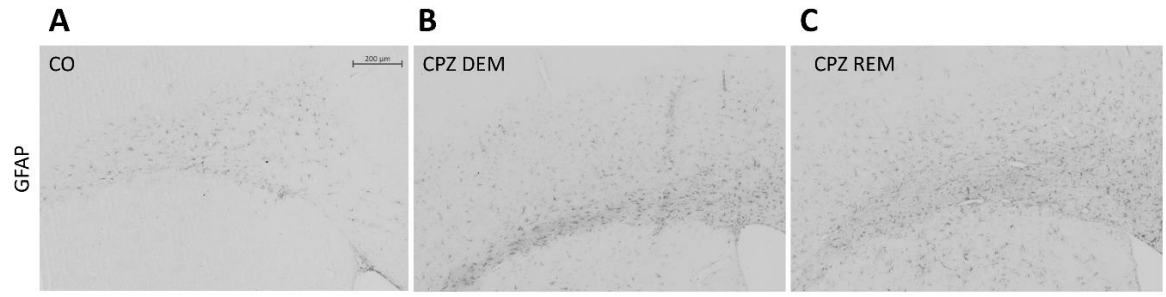

Figure 7. GFAP immunostaining in the area of the corpus callosum of the CO (A), CPZ DEM (B) and CPZ REM (C) group. In the CO group (A) only a small number of astrocytes were detected in the area of the corpus callosum. However, during CPZ treatment an extensive astrogliosis was observed in the CPZ group (B), which persisted until the end of the remyelination phase (C). Scale bar: 200 µm. CO: control group, CPZ: cuprizone, DEM: demyelination group, GFAP: glial fibrillary acidic protein, REM: remyelination group.

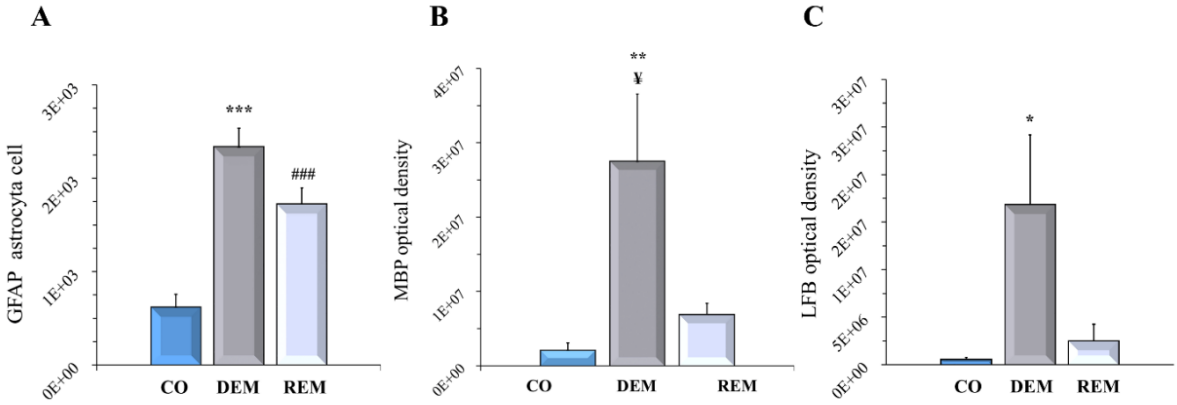

Figure 8. Effect of CPZ administration on myelination of the corpus callosum in the CO, DEM and REM group. Immunohistochemical staining for GFAP (A) in the area of the corpus callosum, where the quantification of astrogliosis was done by manual cell counting. MBP (B) and LFB/CV (C) staining for myelin content determination by intensity measurement. Our results show that the CPZ treatment caused an extensive astrogliosis and a significant decrease in myelin content in the CPZ-treated group compared to the CO group. CO: control group, DEM: demyelination group, GFAP: glial fibrillary acidic protein, LFB/CV: luxol fast blue - cresyl violet, MBP: myelin basic protein, REM: remyelination group, *: $p < 0.05$ vs. CO, **: $p < 0.01$ vs. CO, ¥: $p < 0.05$ vs. REM, ***: $p < 0.001$ vs. CO, ###: $p < 0.001$ vs. CO. The data are presented as mean ± SEM.

Behavioral analyzes

During the weeks of the CPZ treatment and the recovery phase, no significant differences were observed between the CPZ- and CO groups in any of the measured parameters in either the open field test **(Figure 9)**, or in the rotarod test **(Figure 10)**.

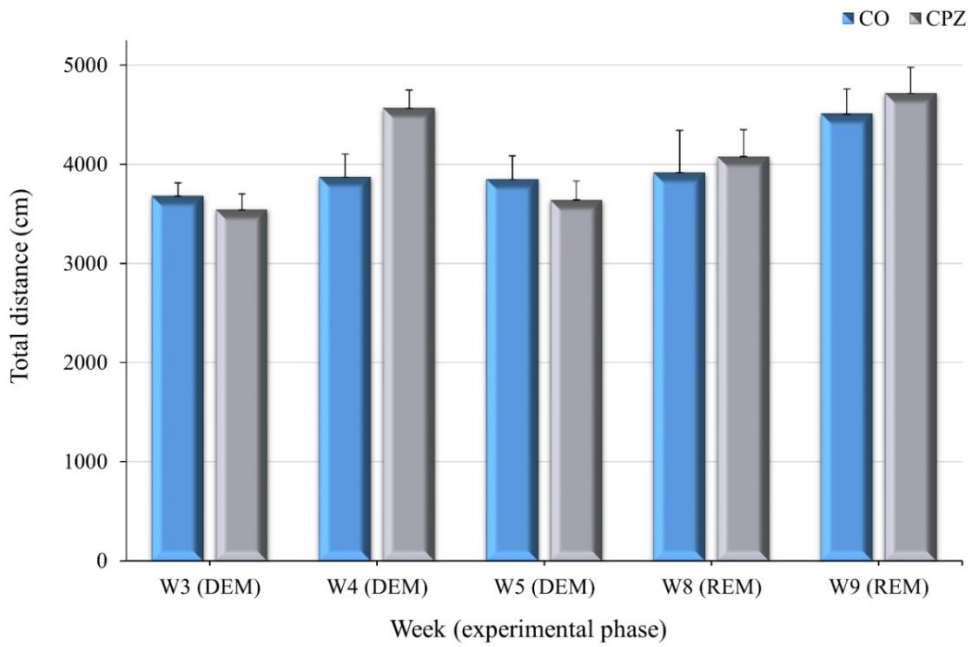

Figure 9. Results of the open field behavioral analyze. Data are presented as the total ambulation distance in the CO, CPZ DEM and CPZ REM groups. CO: control group, CPZ: cuprizone treated group, DEM: demyelination phase in the treated group, REM: remyelination phase in the treated group, W: week, n = 18/group. The data are presented as mean ± SEM.

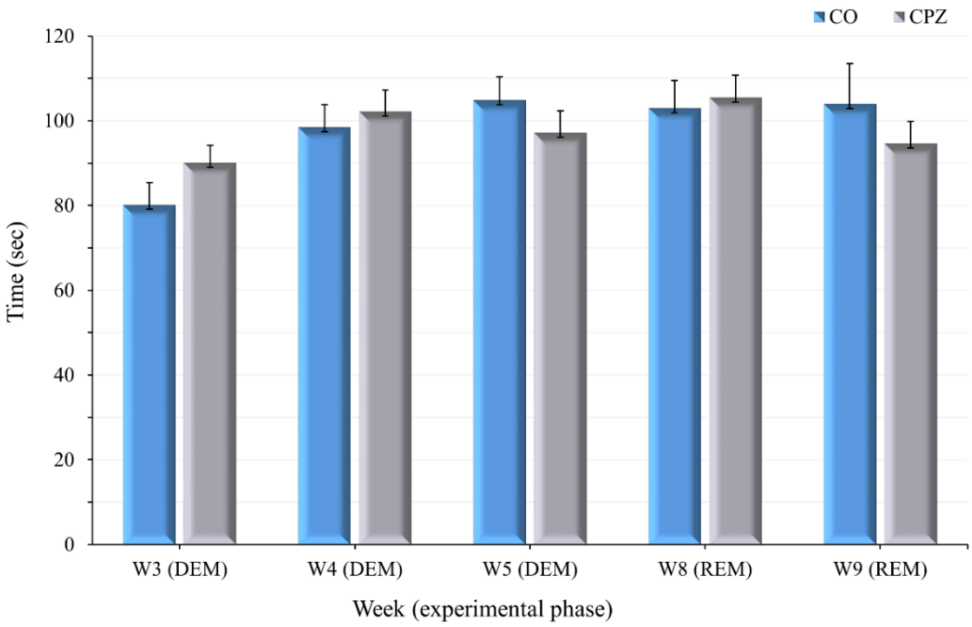

Figure 10. Result of the rotarod behavioral test. Data are presented as the total time spent on the rod in the CO, CPZ DEM and CPZ REM groups. CO: control group, CPZ: cuprizone treated group, DEM: demyelination phase of the treated group, REM: remyelination phase of the treated group, W: week, n = 18/group. The data are presented as mean ± SEM.

Determination of tryptophan metabolites by HPLC analyses from brain and plasma samples

During the bioanalytical measurements, we examined the differences in serotonin (5-HT), TRP, KYN and KYNA concentrations in five brain regions, including the somatosensory cortex, hippocampus, striatum, cerebellum and brainstem. At the end of the demyelination phase, a significant decrease in KYNA concentration was observed in the plasma **(Figure 11A)**, hippocampus **(Figure 11B)** and cortex **(Figure 11C)**, which differences disappeared by the 4th week of remyelination period, between CPZ-treated and CO groups. As the data distribution was not normal ($p > 0.05$), data were presented as mean (1st and 3rd quartile range). The boxplots represent only the significant changes observed after the sample measurements, the other three metabolites (TRP, KYN and serotonin (5-HT)) did not change significantly in the assessed brain regions.

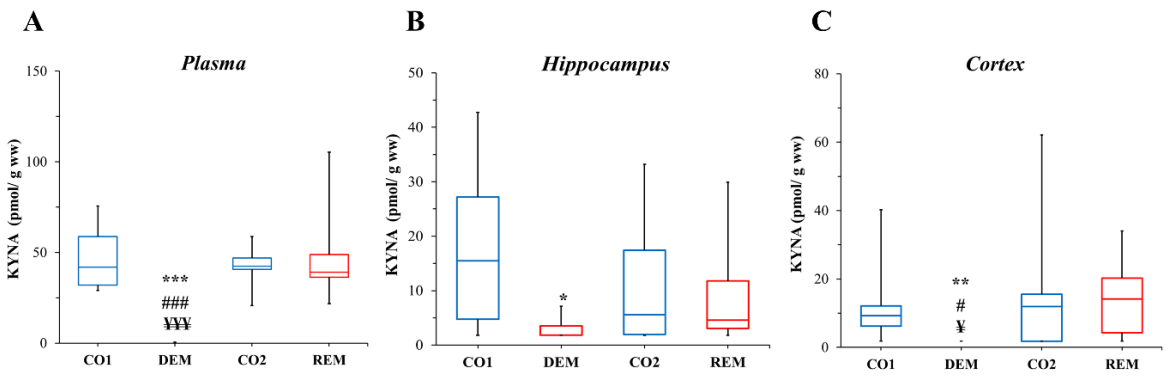

Figure 11. Decreased levels of kynurenic acid in the CPZ-treated group (demyelination group) in plasma and brain regions. n = 10/group, except DEM, where one animal died in cage after anesthesia. CO1: age-matched control group belonging to the CPZ-treated group (DEM) in the demyelination phase; CO2: age-matched control group in the remyelination phase, CPZ: cuprizone; DEM: demyelination phase of the treated group, KYNA: kynurenic acid, REM: remyelination phase of the treated group, ww: wet weight. *: $p < 0.05$ vs. CO1, **: $p < 0.01$ vs. CO1, ***: $p < 0.001$ vs. CO1, #: $p < 0.05$ vs. CO2, ###: $p < 0.001$ vs. CO2, ¥: $p < 0.05$ vs. REM, ¥¥¥: $p < 0.001$ vs. REM.

II. Mapping of metabolites concentration involved in the kynurenine pathway TRP metabolism in the CPZ-induced rodent model

Body weight measurement

Already in the first few days of CPZ treatment, a significant decrease was observed in the body weight of the intoxicated animals compared to the CO, which remained unchanged until the end of the demyelination period and at the beginning of the recovery phase. However, during the remyelination period, this difference showed a decreasing trend and then disappeared. Finally, at the end of the investigation, the body weight of the CO and the CPZ-treated group were in the same range **(Figure 12)**.

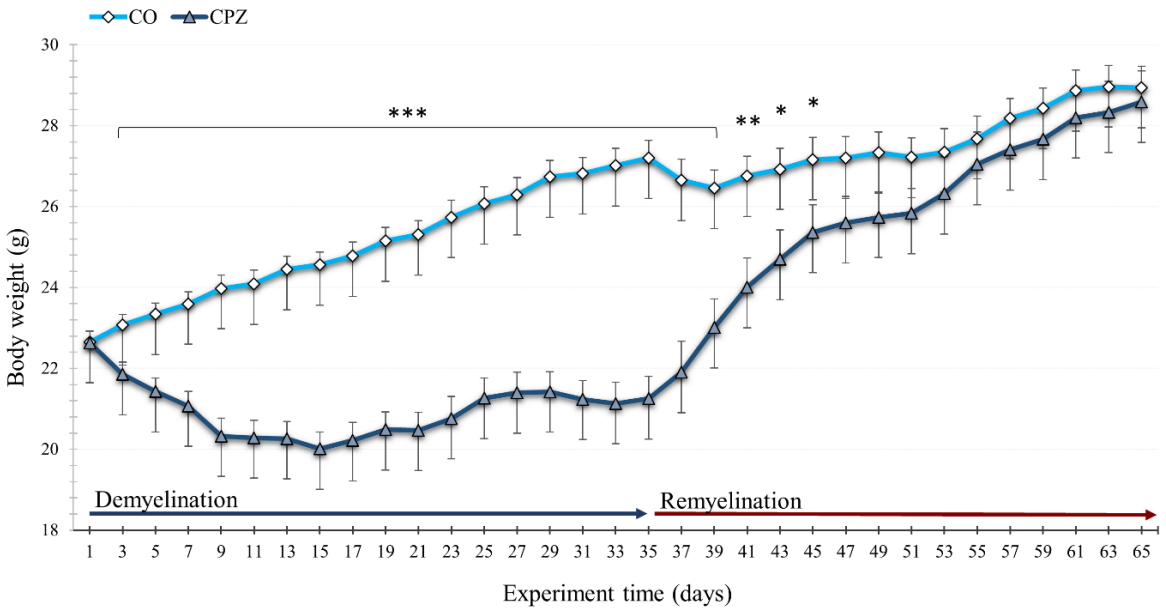

Figure 12. Differences in body weight of animals during investigation. The CO group is depicted with white diamonds and CPZ toxin treated group is depicted with gray triangles. The demyelination and remyelination period are indicated with blue and red arrows. CO: control group; CPZ: cuprizone treated group, *: $p < 0.05$ vs. CO, **: $p < 0.01$ vs. CO, ***: $p < 0.001$ vs. CO. The data are presented as mean ± SEM.

Determination of myelin damage caused by cuprizone toxin treatment

Myelin damage was examined by LFB/CV immunostaining. As a result of poisoning caused by the CPZ toxin, a significant reduction of myelin in the corpus callosum area was visible in the 3rd week of treatment, and the demyelination was even more extensive in the 5th week of CPZ treatment. However, in the 2nd week of the recovery phase, there were no more signs of myelin damage on the brain slices **(Figure 13)**, meaning that the remyelination proved to be effective.

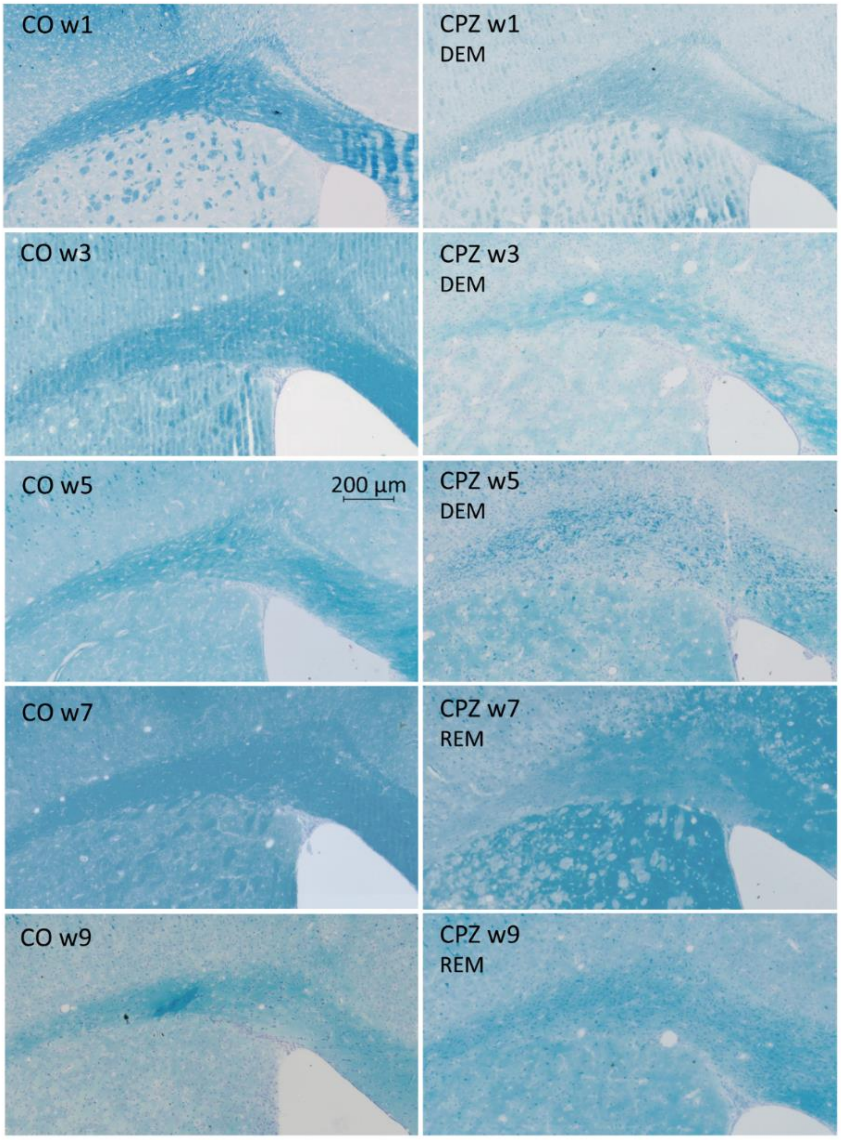

Figure 13. Luxol fast blue - cresyl violet immunostaining in the corpus callosum area of the CO and CPZ treated groups in the 1st, 3rd and 5th, week of CPZ intoxication (DEM), and in the 2nd and 4th weeks of the remyelination phase (REM), which is the 7th and 9th weeks of the examination. In the 3rd week of treatment, a significant decrease in myelin content was observed in CPZ-treated group (CPZ w3 vs. CO w3), compared to the CO, which became even more pronounced by week 5th of poisoning (CPZ w5 vs. CO w5). However, after the animals stopped consuming the CPZ, no significant differences were seen between the groups in the remyelination period (CPZ w7 vs. CO w7; CPZ w9 vs. CO w9). Scale bar: 200 µm. CO: control group; CPZ: cuprizone-treated group; DEM: demyelination phase in the treated group; LFB/CV: luxol fast blue - cresyl violet; REM: remyelination phase in the treated group; w: week

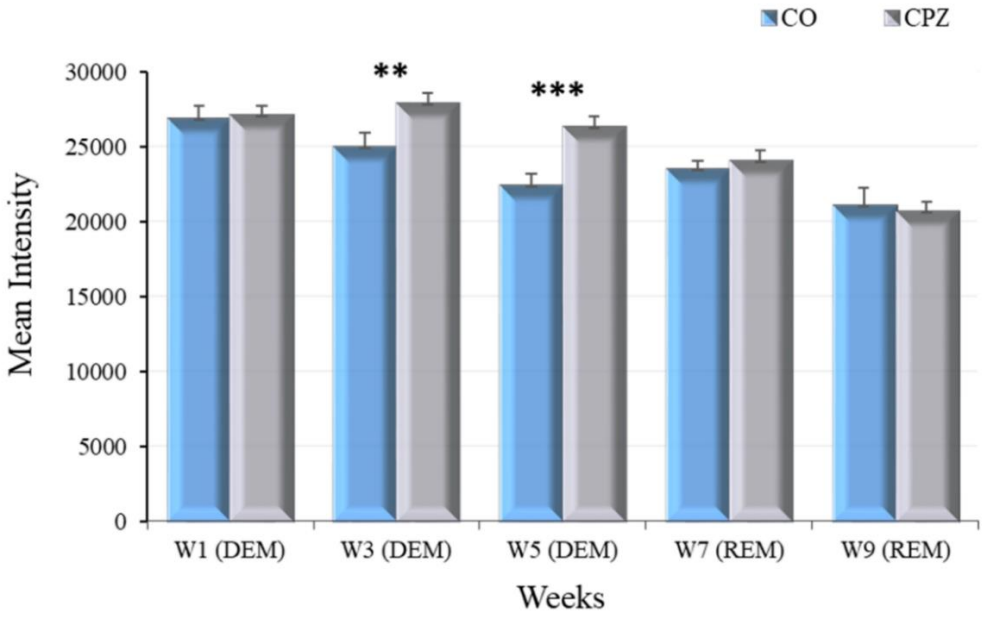

Figure 14. Determination the degree of demyelination caused by CPZ treatment in the CO and CPZ group. LFB/CV immunostaining for evaluation of myelin content by intensity measurement. In the 3rd and 5th weeks of CPZ intoxication, the CPZ treatment significantly reduced myelin content in the CPZ group compared to the CO (W3 (DEM) and W5 (DEM)). However, in the recovery phase, due to remyelination, this difference quickly disappeared between groups. CC: corpus callosum; CO: control group; CPZ: cuprizone group; LFB/CV: luxol fast blue - cresyl violet; W: week; **: $p < 0.01$ vs. CO; ***: $p < 0.001$ vs. CO. The data are presented as mean ± SEM.

Ultra-High-Performance Liquid Chromatography with Tandem Mass Spectrometry Measurement of Kynurenine Metabolites

In our investigation, using UHPLC-MS/MS bioanalytical measurements, we analyzed the concentration distribution of TRP and different KYN metabolites in plasma samples and five different brain region, including the cortex, hippocampus, striatum, cerebellum, and brainstem. These samples were collected on the 1st, 3rd and 5th week of CPZ treatment, and on the 2nd and 4th week of the remyelination phase.

We observed a significant distinction in the concentration of KYNA, 3-HK, and XA of the plasma samples with regard to the CPZ treatment time and the degree of damage. Because already, at the 1st week of the CPZ treatment, a significant decrease in the level of the metabolites was seen, and differences continued until the end of CPZ treatment. However, in the 2nd week of the remyelination phase, these concentration distinctions vanished while the

concentration of KYNA, 3-HK, and XA was in the same range in both groups in the recovery period **(Figure 15)**.

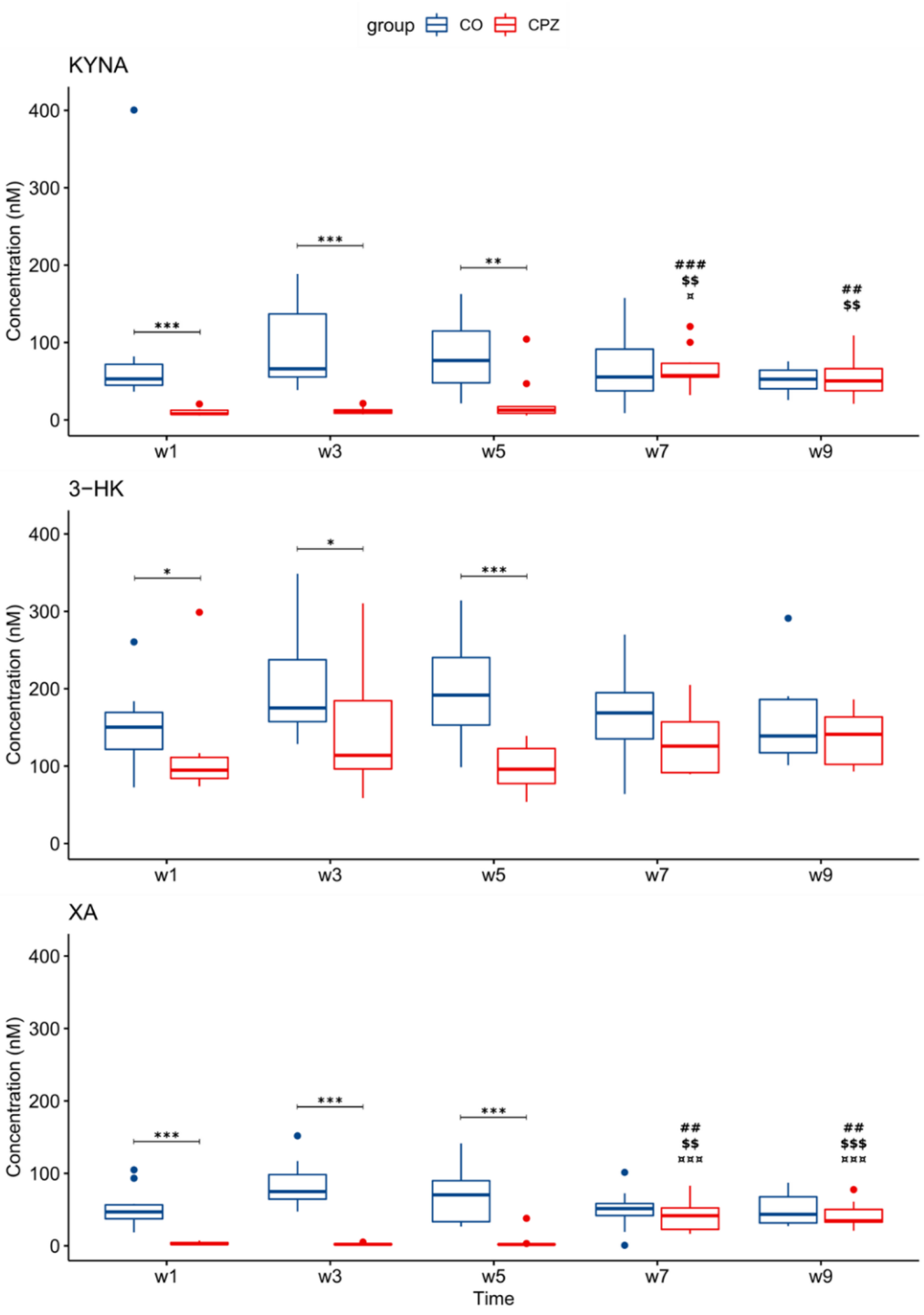

Figure 15. Alterations in the levels of kynurenine metabolites in the plasma of CPZ treated and CO groups. The CPZ treatment caused a significant reduction in KYNA, 3-HK, and XA concentrations in the CPZ group, and this dissimilarity persisted until the end of treatment

(w1, w3 and w5). While the beginning of the remyelination period, these distinctions disappeared between groups (w7 and w9). 3-HK: 3-hydroxy-L-kynurenine; CO: control group; CPZ: cuprizone group; KYNA: kynurenic acid; XA: xanthurenic acid; w: week; *: $p < 0.05$: **: $p < 0.01$; ***: $p < 0.001$: ##: $p < 0.01$; ###: $p < 0.001$ compared to week 1; $$: $p < 0.01$; $$$: $p < 0.001$ compared to week 3; ¤: $p < 0.05$; ¤¤¤: $p < 0.001$ compared to week 5.

Furthermore, in the 5th week of CPZ treatment, we also observed differences in plasma TRP and ANA concentrations, in addition to KYNA, 3-HK and XA, between CPZ and CO groups **(Figure 16)**.

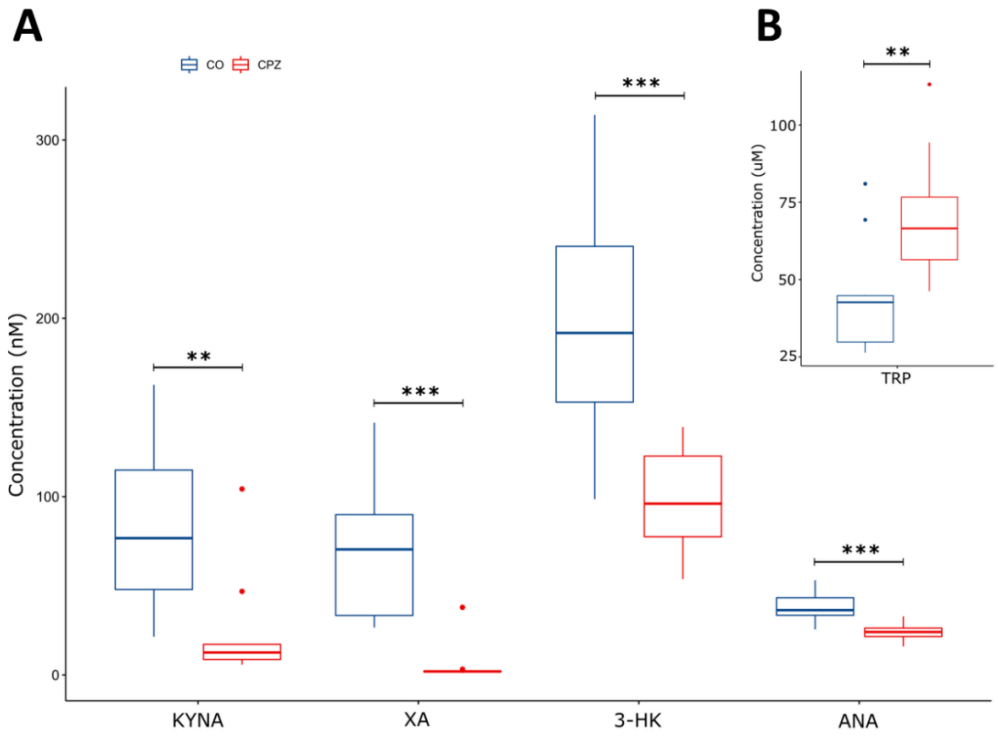

Figure 16. Variations in metabolite levels of plasma samples during the 5th week of CPZ treatment. As a result of intoxication, we observed significant differences in the concentration of KYNA, 3-HK, and XA and ANA (nM) (A), as well as TRP (µM) metabolites (B) between CPZ-treated and CO groups. CO: control group; CPZ: cuprizone group: 3-HK: 3-hydroxy-L-kynurenine; ANA: anthranilic acid; KYNA: kynurenic acid; TRP: tryptophan; XA: xanthurenic acid; w: week; **: $p < 0.01$; ***: $p < 0.001$.

During the examination of the brain regions, a remarkable distinction was noticed in the 3-HK level of the striatum, already in the 1st week of the CPZ treatment. Moreover, in the 3rd week of treatment, in addition to the striatum, a notable decrease in 3-HK level was also observed in the cortex, hippocampus, and brainstem, which continued in the 5th week of intoxication and became even more marked in the cortex and the hippocampus regions **(Figure 17)**.

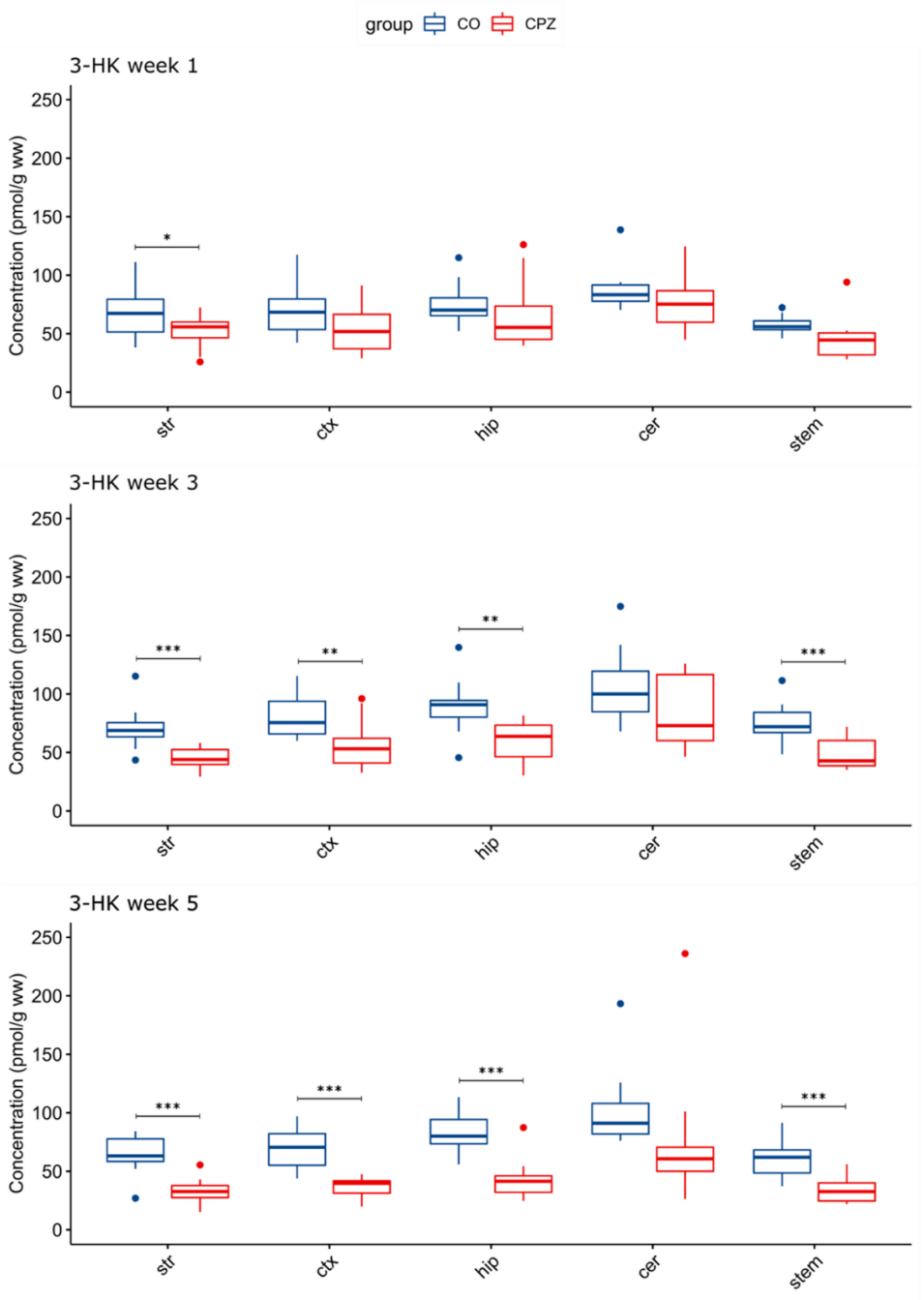

Figure 17. Changes of 3-hydroxy-L-kynurenine levels in some brain regions during CPZ poisoning. As the damage caused by the treatment worsened, there was a notable difference

in 3-HK concentrations between the CPZ and CO groups. 3-HK: 3-hydroxy-L-kynurenine; CO: control group; cer: cerebellum: CPZ: cuprizone group: ctx: cortex; hip: hippocampus; stem: brainstem; str: striatum; ww: wet weight; *: $p < 0.05$; **: $p < 0.01$; ***: $p < 0.001$.

In addition, at the end of the CPZ treatment, we also found a remarkable difference in the ANA concentration in the striatum, cortex, hippocampus, and brainstem of the CPZ-treated compared to the CO group **(Figure 18)**.

Moreover, we found an elevated TRP levels in the cortex and hippocampus in the CPZ group in the 3rd week of demyelination period. Moreover, by the end of the CPZ treatment, we already observed a difference between the CPZ and CO groups in the striatum too, as well as this increased TRP concentration became even more evident in the cortex and the hippocampus by this time **(Figure 19)**.

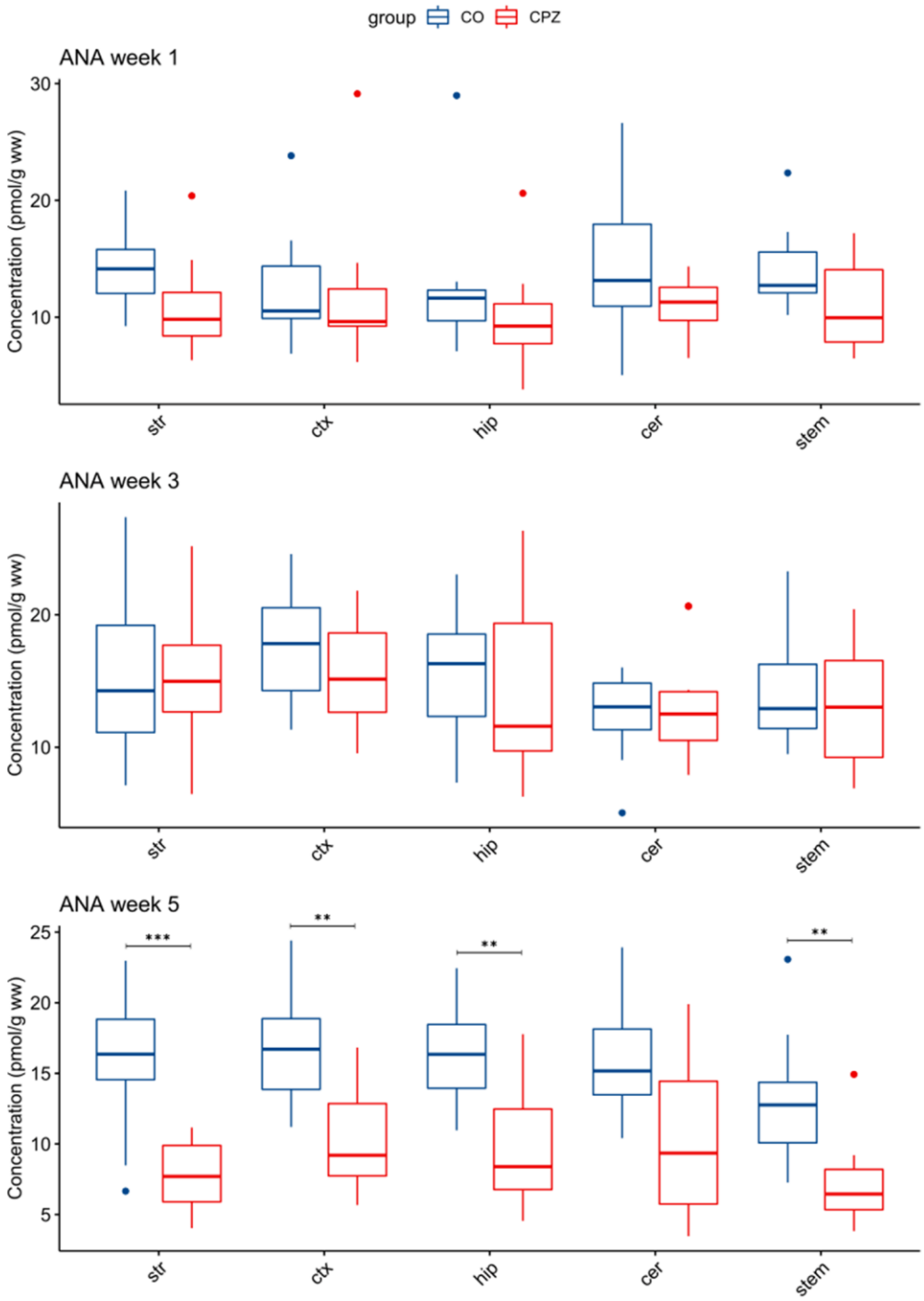

Figure 18. Alterations in ANA levels during intoxication. In the 5th week of poisoning, ANA concentrations were significantly lower in the striatum, cortex, hippocampus, and brainstem in CPZ-treated group, than the control. ANA: anthranilic acid; cer: cerebellum; CO: control group; CPZ: cuprizone group; ctx: cortex; hip: hippocampus; stem: brainstem; str: striatum; ww: wet weight; **: $p < 0.01$; ***: $p < 0.001$.

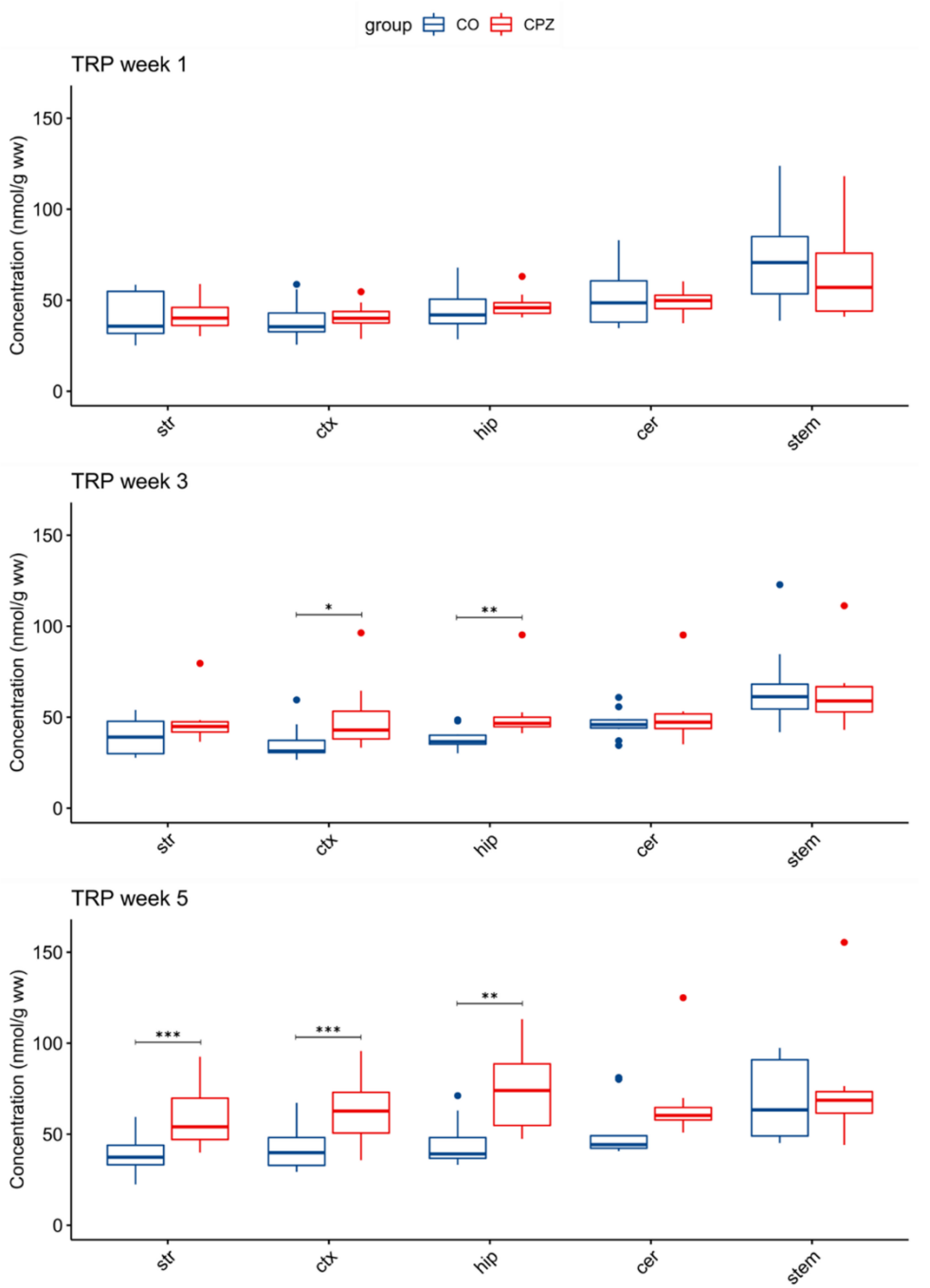

Figure 19. Alterations of TRP levels in certain brain regions during CPZ intoxication. Elevated TRP concentration was observed in the cortex and hippocampus of the CPZ treated group in the 3rd week of intoxication. However, in addition to the cortex and hippocampus, the concentration of TRP also elevated in the striatum of the CPZ group by the 5th week of treatment. cer: cerebellum; CO: control group; CPZ: cuprizone group; ctx: cortex: hip: hippocampus; stem: brainstem: str: striatum; ww: wet weight; TRP tryptophan; *: $p < 0.05$; **: $p < 0.01$; ***: $p < 0.001$.

Discussion

Tryptophan metabolites and multiple sclerosis

The complexity of MS may arise from the different severity and course of this demyelinating disease, as well as from the fact that the specific root cause of MS is still not clear and different mechanisms may influence the development of the damage [74]. MS is one of the most common chronic neurodegenerative disease among young adults. Currently, different therapies are available to treat highly variable courses of MS, but their effectiveness in treating neurodegeneration and disability is limited [74,82]. Recently, several studies have described differences in the concentration of certain metabolites involved in the KP of TRP degradation in various inflammatory and neurodegenerative diseases, including MS [58]. Furthermore, different TRP metabolite concentrations were distinguished in individual subtypes of MS, which suggests that the differences and concentration changes experienced during the course of the disease can even serve as potential biomarkers [58,80]. The degeneration or inflammatory state of the CNS can activate the KP of TRP metabolism, thereby the expression of various neuroactive metabolites. Furthermore, the cytokines, which play an important role in inflammatory and immune processes, contribute significantly to the pathogenesis of MS. On the one hand, an elevated level of pro-inflammatory cytokines, as tumor necrosis factor alpha or interferon-gamma has been described before and during relapse period in the RRMS compared to the control, while in the remission phase, the level of anti-inflammatory cytokines increased [83]. Pro-inflammatory cytokines increase IDO expression, which activates the KP [84]. Elevated IDO activity has been experienced, via the KYN/TRP ratio during relapse in RRMS, but not in remission phase [85]. Furthermore, the higher KYNA/QUIN ratio is associated with disease progression, because the level of QUIN increases as the disease worsens, while the KYNA concentration is much lower [75,86]. KP activation can regulate 5-HT expression by depletion of TRP, because a low 5-HT level was found in MS patients compared to the control, which may have associated with disability in the RRMS. Moreover, seasonal lack of 5-HT-derived melatonin is related with relapses in MS, as melatonin plays an important role in the process of remyelination, via its antioxidant and anti-inflammatory effects [84,87].

Regarding the pathophysiology of the KP shift, it is very important to emphasize the function of receptors signaling, the systemic changes of metabolites, or the tissue-specific expression of KP enzymes [88]. Thus, among the different cell populations of the CNS, as monocytes

and microglia, astrocytes or neurons, some can express all the metabolites of the pathway, while others can only express certain components [60,74,89–91]. Metabolic changes of the KP are not only noticeable in various chronic neurodegenerative diseases, but also between different forms of some disorders, as well as also within them, during the worsening of the disease [75,88]. Even within relapsing-remitting, primary and secondary progressive subtypes of MS, the KP disequilibrium was expressed to a significant extent, and differences in the concentration of TRP and its metabolites were detected in the serum, plasma, CSF and urine samples of MS patients [75,92]. Several studies have established the important regulatory role of TRP metabolism and its metabolites in the proper functioning of the immune system and its effect on immune cells [92]. Regarding TRP metabolism, increased KYN, and 5-hydroxytryptophan (5-HTP) levels were visible in the CSF of SPMS patients, while the QA and QA/KYN ratio are elevated in patients with RRMS [75,93,94]. Furthermore, an elevated ANA, 3-HK and 3-HANA serum levels and KYN/TRP ratio were detected in MS patients [75,93]. However, PICA in the serum sample and melatonin in the blood and urine of RRMS, IDO activity in peripheral blood mononuclear cells, as well as KATI and KATII activity decreased in the plasma of MS patients. Interestingly, KYNA levels are completely different in the plasma, serum or CSF samples of patients MS (for a review, see [92]). In the RRMS form, an increased QUIN level and higher QUIN/KYN and QUIN/KYNA ratios were experienced during acute relapse [93], but the KYNA concentration was lower in the CSF, while it was elevated in plasma [80]. Furthermore, a reduced TRP level was described in the serum and CSF of patients with RRMS compared to the control [80]. However, a higher KYNA concentration was observed in progressive MS, while the KYNA level was lower during remission [58,75,86]. Tömösi et al described a decreased KYNA and increased QUIN level in CSF and serum of SM patients, which caused a high QUIN/KYNA ratio, while the KYNA/KYN and PICA/QUIN ratio was lower in the MS group than in the control. In addition, the 3-HK level was higher in CSF in the MS patients [80].

Taking into account the shifts and disequilibrium of KP in several chronic, inflammatory and neurodegenerative diseases, it is understandable that the metabolites and enzymes of the pathway can be considered as potential therapeutic targets in many disorders. However, the knowledge resulting from the abnormal deviations of KP in some subtypes of the diseases is still limited. Therefore, it is essential to map and understand the pathophysiological processes behind the imbalance of the KP in order to develop targeted therapies.

Metabolites of the tryptophan breakdown and cuprizone rodent model

In the recent decades, MS and its CPZ toxin-induced demyelination animal model have been widely researched. This is not surprising, since many mechanisms have been identified that can be linked to damage processes and neurodegeneration, as well as countless new research results have been published in this field. However, TRP metabolism and its KP have not been the focus of research in the CPZ induced model until now.

Our research group was the first to report the KP deviations in the CPZ mouse model. The model is suitable for modeling the progressive form of MS, as the main histopathological appearance of damage caused by poisoning is very similar to the changes in the lesion pattern of MS types III and IV [54,95,96], which characterized by demyelination, oligodendrocyte apoptosis, as well as microglia and macrophage activation [40].

MS is an extremely complex syndrome with several clinical manifestations. The pathogenesis of the disease is assumed to be initiated by molecular pathways mediated by both the immune system (outside-in model) and neurodegeneration (inside-out model), which processes are not separate from each other, but are important components of the two types, the difference lies in the timing of the two processes [97]. The basis of the "outside-in" hypothesis is the autoimmune inflammation as the primary pathogenesis, which is secondarily followed by myelin damage, while according to the "inside-out" theory, oligodendrocyte injury and myelin damage are the primary, and followed by activation of the inflammatory response as a secondary pathogenesis. Based on the inside-out model, in the years before the symptoms appear, the initial event of the disease is the degradation of oligodendrocytes and myelin damage, and then these processes can cause secondary autoimmune events, causing inflammatory demyelination [97]. The CPZ toxin model is suitable for investigation the inside-out theory, since the treatment results in demyelination gliosis and oligodendrocyte apoptosis, in the absence of a peripheral immune response, possible due to atrophy of some immune organs such as thymus or spleen [40,97,98]. In patients with MS, the role of adaptive immune cells in the pathology of the disease is unquestionable. However, the question arises whether the immune cells primarily cause the pathology, or they only mediate the normal immune response to oligodendrocyte apoptosis and myelin damage, according to the outside-in hypothesis. If the latter is believed to be true, then the search for the identification of the mechanisms behind the damage is crucial, and the necessity of the CPZ model is indisputable

in MS research, since several CPZ studies shed light on demyelination mechanism based primarily on metabolic sensitivity [99–101].

In the CPZ toxin-induced demyelination animal model, we examined in detail the breakdown of tryptophan, the distribution of the various metabolites produced during its metabolism with bioanalytical measurements. Thereby we mapped the distribution of TRP, serotonin and some kynurenine metabolites in plasma samples and in different brain regions, including the areas most affected by damage caused by intoxication; as well as the differences in response to CPZ treatment in the demyelination phase, as well as then in the recovery period during remyelination. In order to ensure the reliability of the CPZ toxin-induced model and the health of the animals, we continuously monitored the body weight of the mice. During the CPZ treatment, the animals' spontaneous locomotor activity and the movement coordination ability were analyzed with various behavioral tests. Furthermore, we determined the degree of damage caused by the treatment in the area of the corpus callosum using immunohistochemical analyses.

During our studies in the CPZ model, we already experienced a significant difference in body weight between CO and CPZ groups at the beginning of the treatment, which exist until the end of the demyelination period, then disappeared during the remyelination phase, and the body weight of the two groups was the same at the end of investigation. In the analysis of the open-field and rotarod behavior tests did not show differences between groups. These results are consistent with literature data, but these are quite controversial [40]. However, our immunohistological analyzes showed a significant degree of demyelination and astrocyte activation in the CPZ-treated group compared to the CO in the 5^{th} week of poisoning. During the analysis of the brain regions and plasma samples using the HLPC technique, we observed a significant decrease in KYNA concentration in the plasma, hippocampus and cortex of the CPZ group, as a result of the treatment, which differences completely disappeared in the recovery phase and the metabolite level of CO and treated animals moved in the same range.

Our histological results, which are consistent with the literature data [21,40], as well as our results obtained with the HPLC technique motivated us to investigate how the metabolic pathway of TRP changes during CPZ treatment and after its withdraw. The samples collected at different times of the CPZ treatment enabled the monitoring of the degree of myelin damage and the change in the concentration of metabolites involved in TRP breakdown.

During the analysis of the histological damage caused by intoxication, there was no difference in the myelin content between the groups in the 1st week of treatment. However, in the 3rd weeks of intoxication, we already experienced significant myelin damage in the group treated with CPZ, which became even more pronounced of the 5th week of poisoning and developed into severe demyelination in the area of the corpus callosum, which condition characterized by significant demyelination, extensive astrogliosis and microgliosis and severe axonal damage [21,40,102].

For bioanalytical measurements, UHPLCMS/MS analysis was used to map the metabolites of TRP degradation. Already at the beginning of the CPZ treatment, we experienced differences in the concentration of the KYNA, XA and 3-HK in the plasma samples, which remained until the end of the intoxication, supplemented by the difference in TRP and ANA levels in the CPZ-treated group, which differences between groups disappeared during remyelination. Oxidative and endoplasmic stress induced by the intoxication together cause significant OLG apoptosis already in the few days after the start of CPZ treatment, and by the 3rd week of poisoning, remarkable demyelination develops, a series of cellular and inflammatory events are activated, which ultimately resulting in demyelination and OLG apoptosis (for a detailed review, see [21]). Moreover, the toxin treatment changes the plasma amino acid level, which may result from abnormal liver function due to megamitochondrium formation [103]. In our studies, as CPZ poisoning progressed, in addition to more pronounced demyelination, we observed differences in body weight and kynurenine metabolite concentration, which quickly disappeared during recovery period, this suggests the effectiveness of the remyelination ability. Not to mention, a significant decrease in ANA and 3-HK concentration and an increase in TRP level during the demyelination phase in the examination of the brain regions, and the normalization of the concentration in the remyelination period. Recently, researchers reported a reduced level of 3-HK among MS patients, which can be linked to microglial activity [76], and it is also known that microglia are the primary main source of 3-HK [104]. In the CPZ-induced model, microglial activation starts already in the first weeks of treatment and continues until the 5th week of demyelination [21,40]. In addition, the blood-brain barrier is important in the distribution of metabolites, TRP and 3-HK easily pass via the blood-brain barrier, unlike KYNA, however, the CPZ treatment does not affect the barrier, it remains relatively intact [21,76,105,106]. Through microglial activation, regulation disorders of TRP-kynurenine metabolism can be associated with neurodegenerative processes [107–109]. The relationship between the alteration of the 3-HK level and microglia activation may arise from

genetic changeability of enzymes, the variety of enzyme activity location, and the resulting differences in the levels of TRP breakdown metabolites [76,110]. Nevertheless, reduced 3-HK levels have been reported in schizophrenic patients [111] and patients with major depressive disorder [112], which diseases can be related with microglia activation [113–115]. Until now, 3-HK has been regarded as a neurotoxic metabolite, because it provokes cell death via diverse excitotoxic processes [107,116]. However, 3-HK is quite a contested metabolite, since in recent years more and more evidence indicates that it is not toxic in all cases. On the one hand, it can act as a scavenger, or with 3-HANA, it can play a role in preventing further damage by regulating the redox balance of the brain tissue, but on the other hand, 3-HK can support oxidative damage depending on the type of cells, pH, and the redox potential [107,117,118].

According to literature data, XA and ANA are known for their antioxidant function. Based on studies, XA is able to bind free radicals and superoxide anion, as well as it also inhibits the inactivation of NADP-isocitrate dehydrogenase by iron, lipid peroxidation, and autooxidation of hematoxylin [118–121]. Similarly, ANA is also an effective free radical scavenger, in addition it can influence the synthesis of non-steroidal anti-inflammatory drugs and respiratory parameters [118,121–123]. Based on these results, ANA and XA may fulfill an antioxidant function during CPZ treatment, thus trying to reduce the oxidative stress. Therefore, certain metabolites in the KP are neuroactive, some of them are neuroprotective or neurotoxic [58]. However, the changes in the concentration of metabolites can be influenced by the activity of the enzymes in the KP. Thus, the increased TRP concentration in the CNS may be caused by a decrease in the activity of the enzyme involved in the downward KP, or by the compensatory mechanisms that provides the availability of TRP metabolite during CPZ poisoning, or by a combination of these two mechanisms. In a study conducted among MS patients, an increased TRP concentration was experienced among patients compared to the control group [124]. Moreover, the enzyme functions of the pathway can also affected by CPZ poisoning. The changes in the copper level have an impact on the functioning of KAT enzymes in the periphery [125], which may explain the differences in plasma KYNA and XA concentrations during intoxication.

Furthermore, as a result of CPZ treatment, the activity of the copper–zinc superoxide dismutase cuproenzyme is also reduced [96,126,127]. The concentration of copper in the body is tightly regulated, therefore any disturbance in its homeostasis causes serious neurodegeneration [21]. Copper has an important role in many cellular processes [21], and it

is a cofactor for different copper enzymes, such as monoamine oxidase [128], superoxide dismutase [129], the cytochrome c oxidase family [130], dopamine-hydroxylase [131], as well as cytochrome c oxidase assembly protein [132,133]. In addition, CPZ treatment also provoked a serious disturbance in neurotransmitter homeostasis [21]. It regulates the function of glutamic acid decarboxylase, thus influencing glutamate and gamma-aminobutyric acid concentrations [134,135], and also has an effect on the levels of norepinephrine and dopamine through the regulation of dopamine hydroxylase and monoamine oxidase [21,133,136].

During our investigation, we observed a significant decrease in the levels of 3-HK and ANA, as well as an increase in the concentration of TRP metabolite in certain brain regions of the toxin-treated group, including the striatum, hippocampus, cortex and brainstem, which areas are referred to in the literature as severely demyelinated brain regions during CPZ intoxication [40], since the oligodendrocytosis caused by the toxin is unevenly distributed in the CNS [40], as well as the dry matter mass of the brain also decreases as a results of CPZ treatment [21]. Thus the differences in the volume of the mentioned brain areas may be linked to the differences in metabolite levels experienced in certain regions.

In the present study, we confirmed the involvement of the metabolic pathway of TRP degradation in the CPZ rodent model. Based on the differences in the KP and the changes in some metabolite concentrations, further questions appear as to the mechanisms behind these shifts. It may happen that CPZ poisoning affects the functions of certain enzymes in the KP, thereby affecting the metabolite concentrations; or some neuroprotective metabolites are used up due to their beneficial effect. Thus reducing the degree of damage and helping remyelination, but a compensatory mechanism may also arise in the background; or perhaps completely different processes from these. Nevertheless, the exact role and effect of the metabolic breakdown of the TRP in the CPZ demyelination model may be clarified by conducting further research.

Overall, in our investigation, during HPLC and UHPLC-MS/MS bioanalytical measurements, we experienced a significant decrease in the plasma KYNA, 3-HK, XA and ANA concentrations of the CPZ-treated group, as well as we observed a notable increase in the TRP level as a result of the CPZ poisoning **(Figure 20)**. However, we were unable to reproduce the reduced KYNA concentration obtained with the HPLC method in the mentioned regions by UHPLC-MS/MS analysis. One of the possible reasons for this is the different sample preparation processes (precipitation with perchloric acid/ acetonitrile) of the various bioanalytical measurement methods applied during our studies, and the detection methods are

also dissimilar (UV–VIS/ UHPLC-MS/MS). Unlike fluorescent detectors, KYNA can be measured in brain samples in a much narrower concentration range with the UHPLC-MS/MS method [137]. Nevertheless, as a result of CPZ intoxication, a remarkable decrease in the levels of 3-HK and ANA was observed in several brain regions, including striatum, cortex, hippocampus and brainstem, while the concentration of TRP increased in the striatum, cortex and hippocampus of CPZ-treated animals compared to the control group **(Figure 20)**.

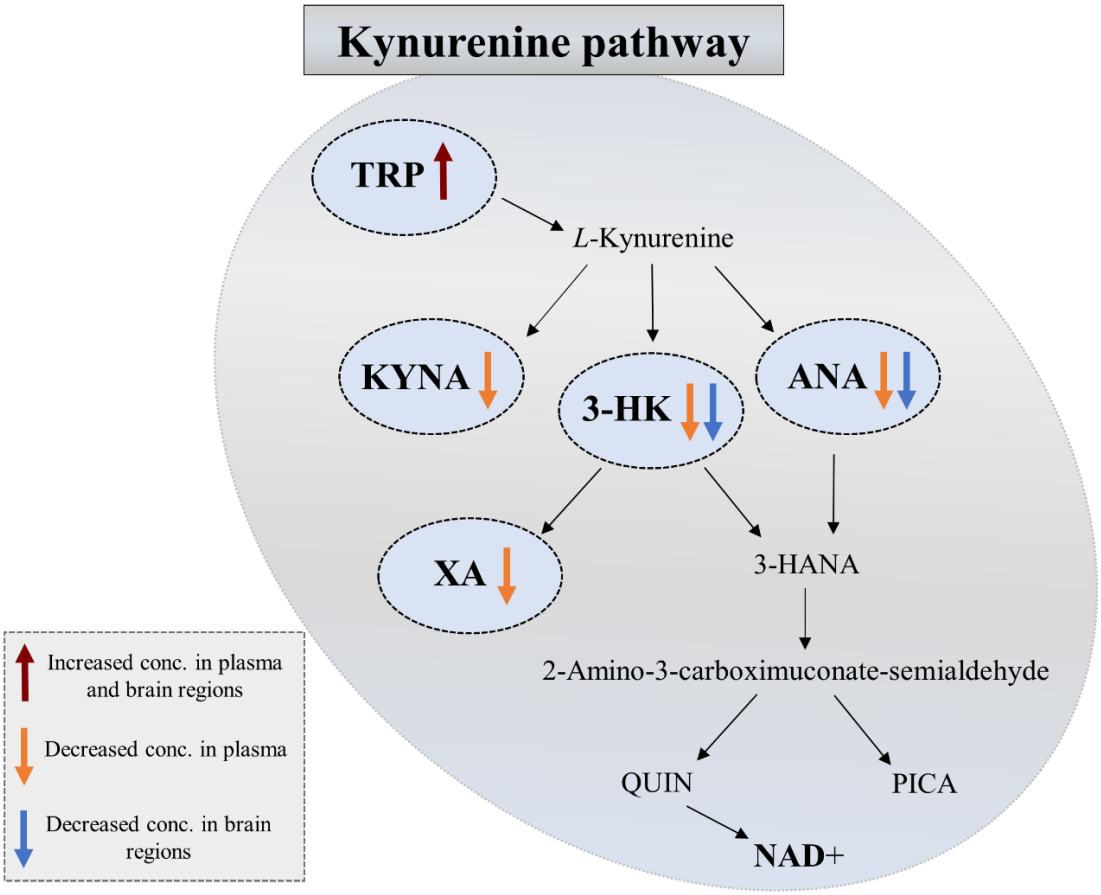

Figure 20. Alterations in kynurenine pathway metabolite concentrations in plasma and certain brain regions in response to cuprizone treatment. As a result of intoxication elevated TRP concentration was observed in the plasma, striatum, cortex and hippocampus of the CPZ treated animals. Furthermore, reduced KYNA, 3-HK, XA and ANA plasma concentrations were experienced, as well as decreased 3-HK and ANA levels were visible in the striatum, cortex hippocampus and brainstem of CPZ treated group compared to the control group during intoxication. 3-HANA: 3-hydroxyanthranilic acid; 3-HK: 3-hydroxy-L-kynurenine; ANA: anthranilic acid; KYNA: kynurenic acid; NAD^+: nicotinamide adenine dinucleotide; PICA: picolinic acid; TRP: tryptophan; XA: xanthurenic acid; QUIN: quinolinic acid

Conclusion

Our study, conducted in the CPZ toxin-induced demyelination animal model, was the first to report in full detail the kynurenine metabolite profile of TRP breakdown during progressive demyelination.

In addition to the basic histological analyses, behavioral and physical state assessment, we revealed the involvement of kynurenine metabolites in the processes of damage caused by CPZ poisoning on both sides of the blood-brain barrier and then highlighted the effectiveness of the remyelination ability in the field of TRP metabolism as well.

Our research results can serve as a starting point for further studies, with the help of which we can get even closer to understanding the processes that cause damage and the mechanisms connecting TRP degradation, what role certain metabolites can play in the creation of damage, how they influence the demyelination or remyelination processes. Furthermore, by detecting these processes, we can get a more transparent picture and get closer to discover the pathomechanism of MS.

In the near future, the regulation of the amount of certain metabolites may serve as a possible therapeutic tool in the treatment of MS, as well as may hold potential targets for drug research. Therefore, the research can serve as a basis for the creation of artificially synthesized compounds with new attack points, which may present a new therapeutic option in the treatment of MS.

Acknowledgement

First and foremost, I would like to express my infinite gratitude to my supervisors Professor László Vécsei and Associate Professor Cecilia Rajda for their personal guidance, professional advice and continuous support; and for forming my general view of scientific research since my gratitude years and giving invaluable advice during my work.

I would like to thank Professor Péter Klivényi for providing me the possibility and the background for my research activity.

From all my colleagues, I would like to express my gratitude to my friend Dr. Edina Katalin Veréb for teaching me to define the research problems and to solve them, for ongoing supports, encouragements and suggestions.

I would also like to thank to all my colleagues, with whom I performed the research work, especially my closest colleagues and friends Orsolya Horváth M.Sc., Diána Martos M.Sc. and Dr. Nikolett Nánási for support, conversations and for helping me during my research years.

I wish to extend my gratitude towards my others colleagues Dr. Zsolt Galla, Dr. Zsuzsanna Fülöpné Bohár, Associate Professor Dénes Zádori, and Dr. Gábor Veres, for helping me my research work.

I express my gratitude towards Orsolya Ivánkovitsné Kiss, Krisztina Fülöp for their valuable professional help and for showing me the technical parts of the laboratory work.

My special thanks are due to my all friends, who have been always by my side.

Last, but not least, I would like to express my special thank and endless gratitude to my beloved family for their unconditional love, continuous support, for always being there for me and believing in me during all these years.

I would also like to acknowledge all the financial support during my all research work, which was given by the grants GINOP-2.3.2-15-2016-00034, EFOP-3.6.1-16-2016-00008, National Research, Development, and Innovation Office–NKFIH K138125, ÚNKP-20/21/22/23-3-New National Excellence Program of the Ministry for Innovation and Technology from the source of the National Research, Development and Innovation Fund; and EFOP 3.6.3-VEKOP-16-2017-00009. At the time of my research years, I was partly supported by the Doctoral School of Clinical Medicine, Albert Szent-Györgyi Medical School, University of Szeged.

References

[1] Benedict RHB, Amato MP, DeLuca J, Geurts JJG. Cognitive impairment in multiple sclerosis: clinical management, MRI, and therapeutic avenues. Lancet Neurol 2020;19:860–71. https://doi.org/10.1016/S1474-4422(20)30277-5.

[2] Dobson R, Giovannoni G. Multiple sclerosis – a review. European Journal of Neurology 2019;26:27–40. https://doi.org/10.1111/ene.13819.

[3] Moles L, Egimendia A, Osorio-Querejeta I, Iparraguirre L, Alberro A, Suárez J, et al. Gut Microbiota Changes in Experimental Autoimmune Encephalomyelitis and Cuprizone Mice Models. ACS Chem Neurosci 2021;12:893–905. https://doi.org/10.1021/acschemneuro.0c00695.

[4] Gaetani L, Boscaro F, Pieraccini G, Calabresi P, Romani L, Di Filippo M, et al. Host and Microbial Tryptophan Metabolic Profiling in Multiple Sclerosis. Front Immunol 2020;11:157. https://doi.org/10.3389/fimmu.2020.00157.

[5] Kipp M, Nyamoya S, Hochstrasser T, Amor S. Multiple sclerosis animal models: a clinical and histopathological perspective. Brain Pathology 2017;27:123–37. https://doi.org/10.1111/bpa.12454.

[6] Frohman EM, Racke MK, Raine CS. Multiple sclerosis--the plaque and its pathogenesis. N Engl J Med 2006;354:942–55. https://doi.org/10.1056/NEJMra052130.

[7] Lassmann H, Bradl M. Multiple sclerosis: experimental models and reality. Acta Neuropathol 2017;133:223–44. https://doi.org/10.1007/s00401-016-1631-4.

[8] Karussis D, Karageorgiou C, Vaknin-Dembinsky A, Gowda-Kurkalli B, Gomori JM, Kassis I, et al. Safety and immunological effects of mesenchymal stem cell transplantation in patients with multiple sclerosis and amyotrophic lateral sclerosis. Arch Neurol 2010;67:1187–94. https://doi.org/10.1001/archneurol.2010.248.

[9] Walton C, King R, Rechtman L, Kaye W, Leray E, Marrie RA, et al. Rising prevalence of multiple sclerosis worldwide: Insights from the Atlas of MS, third edition. Mult Scler 2020;26:1816–21. https://doi.org/10.1177/1352458520970841.

[10] Kobelt G, Thompson A, Berg J, Gannedahl M, Eriksson J. New insights into the burden and costs of multiple sclerosis in Europe. Mult Scler 2017;23:1123–36. https://doi.org/10.1177/1352458517694432.

[11] Calandri E, Graziano F, Borghi M, Bonino S. Young adults' adjustment to a recent diagnosis of multiple sclerosis: The role of identity satisfaction and self-efficacy. Disability and Health Journal 2019;12:72–8. https://doi.org/10.1016/j.dhjo.2018.07.008.

[12] Scazzone C, Agnello L, Bivona G, Lo Sasso B, Ciaccio M. Vitamin D and Genetic Susceptibility to Multiple Sclerosis. Biochem Genet 2021;59:1–30. https://doi.org/10.1007/s10528-020-10010-1.

[13] Golden LC, Voskuhl R. The Importance of Studying Sex Differences in Disease: The Example of Multiple Sclerosis. J Neurosci Res 2017;95:633–43. https://doi.org/10.1002/jnr.23955.

[14] Ramagopalan SV, Yee IM, Dyment DA, Orton S-M, Marrie RA, Sadovnick AD, et al. Parent-of-origin effect in multiple sclerosis. Neurology 2009;73:602–5. https://doi.org/10.1212/WNL.0b013e3181af33cf.

[15] Arneth B. Multiple Sclerosis and Smoking. The American Journal of Medicine 2020;133:783–8. https://doi.org/10.1016/j.amjmed.2020.03.008.

[16] Ascherio A, Munger KL. Epidemiology of Multiple Sclerosis: From Risk Factors to Prevention—An Update. Semin Neurol 2016;36:103–14. https://doi.org/10.1055/s-0036-1579693.

[17] Shiri E, Pasbakhsh P, Borhani-Haghighi M, Alizadeh Z, Nekoonam S, Mojaverrostami S, et al. Mesenchymal Stem Cells Ameliorate Cuprizone-Induced Demyelination by Targeting Oxidative Stress and Mitochondrial Dysfunction. Cell Mol Neurobiol 2021;41:1467–81. https://doi.org/10.1007/s10571-020-00910-6.

[18] Rajda C, Pukoli D, Bende Z, Majláth Z, Vécsei L. Excitotoxins, Mitochondrial and Redox Disturbances in Multiple Sclerosis. Int J Mol Sci 2017;18. https://doi.org/10.3390/ijms18020353.
[19] Høglund RA, Maghazachi AA. Multiple sclerosis and the role of immune cells. World J Exp Med 2014;4:27–37. https://doi.org/10.5493/wjem.v4.i3.27.
[20] Ponath G, Park C, Pitt D. The Role of Astrocytes in Multiple Sclerosis. Front Immunol 2018;9:217. https://doi.org/10.3389/fimmu.2018.00217.
[21] Praet J, Guglielmetti C, Berneman Z, Van der Linden A, Ponsaerts P. Cellular and molecular neuropathology of the cuprizone mouse model: clinical relevance for multiple sclerosis. Neurosci Biobehav Rev 2014;47:485–505. https://doi.org/10.1016/j.neubiorev.2014.10.004.
[22] Polyák H, Cseh EK, Bohár Z, Rajda C, Zádori D, Klivényi P, et al. Cuprizone markedly decreases kynurenic acid levels in the rodent brain tissue and plasma. Heliyon 2021;7:e06124. https://doi.org/10.1016/j.heliyon.2021.e06124.
[23] Trenova, A.G., Slavov, G.S., 2015. Cytokines in multiple sclerosis – possible targets for immune therapies. J. Neurol. Exp. Neurosci, Volume 1 Issue 2
[24] Ortiz, G.G., Pacheco-Moises, F., Torres-S_anchez, E., Sorto-G_omez, T., Mireles-Ramírez, M., Le_on-Gil, A., Gonzalez-Usigli, H., Alvarado, L., Gonz_alez, E., S_anchez-L_opez, A., Cid-Hern_andez, M., Vel_azquez-Brizuela, I., 2016. Multiple Sclerosis and its Relationship with Oxidative Stress, Glutathione Redox System, ATPase System, and Membrane Fluidity, Trending topics in Multiple Sclerosis.
[25] Doshi A, Chataway J. Multiple sclerosis, a treatable disease. Clin Med (Lond) 2016;16:s53–9. https://doi.org/10.7861/clinmedicine.16-6s-s53.
[26] Lublin FD, Reingold SC, Cohen JA, Cutter GR, Sørensen PS, Thompson AJ, et al. Defining the clinical course of multiple sclerosis. Neurology 2014;83:278–86. https://doi.org/10.1212/WNL.0000000000000560.
[27] Compston A, Coles A. Multiple sclerosis. Lancet 2008;372:1502–17. https://doi.org/10.1016/S0140-6736(08)61620-7.
[28] Lassmann H, Brück W, Lucchinetti CF. The Immunopathology of Multiple Sclerosis: An Overview. Brain Pathology 2007;17:210–8. https://doi.org/10.1111/j.1750-3639.2007.00064.x.
[29] Lassmann H, van Horssen J, Mahad D. Progressive multiple sclerosis: pathology and pathogenesis. Nat Rev Neurol 2012;8:647–56. https://doi.org/10.1038/nrneurol.2012.168.
[30] Eriksson M, Andersen O, Runmarker B. Long-term follow up of patients with clinically isolated syndromes, relapsing-remitting and secondary progressive multiple sclerosis. Mult Scler 2003;9:260–74. https://doi.org/10.1191/1352458503ms914oa.
[31] Lublin FD. New multiple sclerosis phenotypic classification. Eur Neurol 2014;72 Suppl 1:1–5. https://doi.org/10.1159/000367614.
[32] Mahad DH, Trapp BD, Lassmann H. Pathological mechanisms in progressive multiple sclerosis. The Lancet Neurology 2015;14:183–93. https://doi.org/10.1016/S1474-4422(14)70256-X.
[33] Miller DH, Leary SM. Primary-progressive multiple sclerosis. Lancet Neurol 2007;6:903–12. https://doi.org/10.1016/S1474-4422(07)70243-0.
[34] Kappos L, Wolinsky JS, Giovannoni G, Arnold DL, Wang Q, Bernasconi C, et al. Contribution of Relapse-Independent Progression vs Relapse-Associated Worsening to Overall Confirmed Disability Accumulation in Typical Relapsing Multiple Sclerosis in a Pooled Analysis of 2 Randomized Clinical Trials. JAMA Neurol 2020;77:1–9. https://doi.org/10.1001/jamaneurol.2020.1568.
[35] Tur C, Carbonell-Mirabent P, Cobo-Calvo Á, Otero-Romero S, Arrambide G, Midaglia L, et al. Association of Early Progression Independent of Relapse Activity With Long-term Disability After a First Demyelinating Event in Multiple Sclerosis. JAMA Neurol 2023;80:151–60. https://doi.org/10.1001/jamaneurol.2022.4655.
[36] Prosperini L, Ruggieri S, Haggiag S, Tortorella C, Pozzilli C, Gasperini C. Prognostic Accuracy of NEDA-3 in Long-term Outcomes of Multiple Sclerosis. Neurol Neuroimmunol Neuroinflamm 2021;8:e1059. https://doi.org/10.1212/NXI.0000000000001059.

[37] Cree BAC, Hollenbach JA, Bove R, Kirkish G, Sacco S, Caverzasi E, et al. Silent progression in disease activity–free relapsing multiple sclerosis. Ann Neurol 2019;85:653–66. https://doi.org/10.1002/ana.25463.

[38] Bsteh G, Hegen H, Altmann P, Auer M, Berek K, Pauli FD, et al. Retinal layer thinning is reflecting disability progression independent of relapse activity in multiple sclerosis. Mult Scler J Exp Transl Clin 2020;6:2055217320966344. https://doi.org/10.1177/2055217320966344.

[39] Hauser SL, Cree BAC. Treatment of Multiple Sclerosis: A Review. Am J Med 2020;133:1380-1390.e2. https://doi.org/10.1016/j.amjmed.2020.05.049.

[40] Sen MK, Mahns DA, Coorssen JR, Shortland PJ. Behavioural phenotypes in the cuprizone model of central nervous system demyelination. Neurosci Biobehav Rev 2019;107:23–46. https://doi.org/10.1016/j.neubiorev.2019.08.008.

[41] Polyák H, Galla Z, Nánási N, Cseh EK, Rajda C, Veres G, et al. The Tryptophan-Kynurenine Metabolic System Is Suppressed in Cuprizone-Induced Model of Demyelination Simulating Progressive Multiple Sclerosis. Biomedicines 2023;11:945. https://doi.org/10.3390/biomedicines11030945.

[42] Carlton WW. Response of mice to the chelating agents sodium diethyldithiocarbamate, alpha-benzoinoxime, and biscyclohexanone oxaldihydrazone. Toxicol Appl Pharmacol 1966;8:512–21. https://doi.org/10.1016/0041-008x(66)90062-7.

[43] Lassmann H, Bradl M. Multiple sclerosis: experimental models and reality. Acta Neuropathol 2017;133:223–44. https://doi.org/10.1007/s00401-016-1631-4.

[44] Wakabayashi T. Megamitochondria formation - physiology and pathology. J Cell Mol Med 2002;6:497–538. https://doi.org/10.1111/j.1582-4934.2002.tb00452.x.

[45] Dutta R, Chomyk AM, Chang A, Ribaudo MV, Deckard SA, Doud MK, et al. Hippocampal demyelination and memory dysfunction are associated with increased levels of the neuronal microRNA miR-124 and reduced AMPA receptors. Ann Neurol 2013;73:637–45. https://doi.org/10.1002/ana.23860.

[46] Azami Tameh A, Clarner T, Beyer C, Atlasi MA, Hassanzadeh G, Naderian H. Regional regulation of glutamate signaling during cuprizone-induced demyelination in the brain. Annals of Anatomy - Anatomischer Anzeiger 2013;195:415–23. https://doi.org/10.1016/j.aanat.2013.03.004.

[47] Gudi V, Gingele S, Skripuletz T, Stangel M. Glial response during cuprizone-induced de- and remyelination in the CNS: lessons learned. Front Cell Neurosci 2014;8. https://doi.org/10.3389/fncel.2014.00073.

[48] Hiremath MM, Saito Y, Knapp GW, Ting JP-Y, Suzuki K, Matsushima GK. Microglial/macrophage accumulation during cuprizone-induced demyelination in C57BL/6 mice. Journal of Neuroimmunology 1998;92:38–49. https://doi.org/10.1016/S0165-5728(98)00168-4.

[49] Lampron A, Larochelle A, Laflamme N, Préfontaine P, Plante M-M, Sánchez MG, et al. Inefficient clearance of myelin debris by microglia impairs remyelinating processes. J Exp Med 2015;212:481–95. https://doi.org/10.1084/jem.20141656.

[50] Skripuletz T, Hackstette D, Bauer K, Gudi V, Pul R, Voss E, et al. Astrocytes regulate myelin clearance through recruitment of microglia during cuprizone-induced demyelination. Brain 2013;136:147–67. https://doi.org/10.1093/brain/aws262.

[51] Mason JL, Jones JJ, Taniike M, Morell P, Suzuki K, Matsushima GK. Mature oligodendrocyte apoptosis precedes IGF-1 production and oligodendrocyte progenitor accumulation and differentiation during demyelination/remyelination. Journal of Neuroscience Research 2000;61:251–62. https://doi.org/10.1002/1097-4547(20000801)61:3<251::AID-JNR3>3.0.CO;2-W.

[52] Skripuletz T, Gudi V, Hackstette D, Stangel M. De- and remyelination in the CNS white and grey matter induced by cuprizone: the old, the new, and the unexpected. Histol Histopathol 2011;26:1585–97. https://doi.org/10.14670/HH-26.1585.

[53] Kipp M, Clarner T, Dang J, Copray S, Beyer C. The cuprizone animal model: new insights into an old story. Acta Neuropathol 2009;118:723–36. https://doi.org/10.1007/s00401-009-0591-3.

[54] Lucchinetti C, Brück W, Parisi J, Scheithauer B, Rodriguez M, Lassmann H. Heterogeneity of multiple sclerosis lesions: Implications for the pathogenesis of demyelination. Annals of Neurology 2000;47:707–17. https://doi.org/10.1002/1531-8249(200006)47:6<707::AID-ANA3>3.0.CO;2-Q.
[55] Lassmann H, Brück W, Lucchinetti C. Heterogeneity of multiple sclerosis pathogenesis: implications for diagnosis and therapy. Trends in Molecular Medicine 2001;7:115–21. https://doi.org/10.1016/S1471-4914(00)01909-2.
[56] Popescu BFG, Lucchinetti CF. Pathology of demyelinating diseases. Annu Rev Pathol 2012;7:185–217. https://doi.org/10.1146/annurev-pathol-011811-132443.
[57] McMahon EJ, Suzuki K, Matsushima GK. Peripheral macrophage recruitment in cuprizone-induced CNS demyelination despite an intact blood–brain barrier. Journal of Neuroimmunology 2002;130:32–45. https://doi.org/10.1016/S0165-5728(02)00205-9.
[58] Vécsei L, Szalárdy L, Fülöp F, Toldi J. Kynurenines in the CNS: recent advances and new questions. Nat Rev Drug Discov 2013;12:64–82. https://doi.org/10.1038/nrd3793.
[59] Guillemin GJ, Cullen KM, Lim CK, Smythe GA, Garner B, Kapoor V, et al. Characterization of the kynurenine pathway in human neurons. J Neurosci 2007;27:12884–92. https://doi.org//doi.org/10.1523/JNEUROSCI.4101-07.2007.
[60] Guillemin GJ, Smith DG, Smythe GA, Armati PJ, Brew BJ. Expression of the kynurenine pathway enzymes in human microglia and macrophages. Adv Exp Med Biol 2003;527:105–12. https://doi.org/10.1007/978-1-4615-0135-0_12.
[61] Morales-Puerto N, Giménez-Gómez P, Pérez-Hernández M, Abuin-Martínez C, Gil de Biedma-Elduayen L, Vidal R, et al. Addiction and the kynurenine pathway: A new dancing couple? Pharmacology & Therapeutics 2021;223:107807. https://doi.org/10.1016/j.pharmthera.2021.107807.
[62] Hubková B, Valko-Rokytovská M, Čižmárová B, Zábavníková M, Mareková M, Birková A. Tryptophan: Its Metabolism along the Kynurenine, Serotonin, and Indole Pathway in Malignant Melanoma. International Journal of Molecular Sciences 2022;23:9160. https://doi.org/10.3390/ijms23169160.
[63] Melnikov M, Sviridova A, Rogovskii V, Oleskin A, Boziki M, Bakirtzis C, et al. Serotoninergic system targeting in multiple sclerosis: the prospective for pathogenetic therapy. Multiple Sclerosis and Related Disorders 2021;51:102888. https://doi.org/10.1016/j.msard.2021.102888.
[64] Biernacki T, Sandi D, Bencsik K, Vécsei L. Kynurenines in the Pathogenesis of Multiple Sclerosis: Therapeutic Perspectives. Cells 2020;9. https://doi.org/10.3390/cells9061564.
[65] Taleb O, Maammar M, Klein C, Maitre M, Mensah-Nyagan AG. A Role for Xanthurenic Acid in the Control of Brain Dopaminergic Activity. Int J Mol Sci 2021;22:6974. https://doi.org/10.3390/ijms22136974.
[66] Birch PJ, Grossman CJ, Hayes AG. Kynurenate and FG9041 have both competitive and non-competitive antagonist actions at excitatory amino acid receptors. Eur J Pharmacol 1988;151:313–5. https://doi.org/10.1016/0014-2999(88)90814-x.
[67] Kessler M, Terramani T, Lynch G, Baudry M. A glycine site associated with N-methyl-D-aspartic acid receptors: characterization and identification of a new class of antagonists. J Neurochem 1989;52:1319–28.
[68] Zádori D, Klivényi P, Plangár I, Toldi J, Vécsei L. Endogenous neuroprotection in chronic neurodegenerative disorders: with particular regard to the kynurenines. J Cell Mol Med 2011;15:701–17. https://doi.org/10.1111/j.1582-4934.2010.01237.x.
[69] Bohár Z, Toldi J, Fülöp F, Vécsei L. Changing the Face of Kynurenines and Neurotoxicity: Therapeutic Considerations. Int J Mol Sci 2015;16:9772–93. https://doi.org/10.3390/ijms16059772.
[70] Sandi D, Fricska-Nagy Z, Bencsik K, Vécsei L. Neurodegeneration in Multiple Sclerosis: Symptoms of Silent Progression, Biomarkers and Neuroprotective Therapy—Kynurenines Are Important Players. Molecules 2021;26:3423. https://doi.org/10.3390/molecules26113423.

[71] Guillemin GJ. Quinolinic acid, the inescapable neurotoxin. FEBS J 2012;279:1356–65. https://doi.org/10.1111/j.1742-4658.2012.08485.x.
[72] Zádori D, Klivényi P, Vámos E, Fülöp F, Toldi J, Vécsei L. Kynurenines in chronic neurodegenerative disorders: future therapeutic strategies. J Neural Transm 2009;116:1403–9. https://doi.org/10.1007/s00702-009-0263-4.
[73] Sandi D, Biernacki T, Szekeres D, Füvesi J, Kincses ZT, Rózsa C, et al. Prevalence of cognitive impairment among Hungarian patients with relapsing-remitting multiple sclerosis and clinically isolated syndrome. Multiple Sclerosis and Related Disorders 2017;17:57–62. https://doi.org/10.1016/j.msard.2017.06.017.
[74] Lovelace MD, Varney B, Sundaram G, Franco NF, Ng ML, Pai S, et al. Current Evidence for a Role of the Kynurenine Pathway of Tryptophan Metabolism in Multiple Sclerosis. Front Immunol 2016;7. https://doi.org/10.3389/fimmu.2016.00246.
[75] Lim CK, Bilgin A, Lovejoy DB, Tan V, Bustamante S, Taylor BV, et al. Kynurenine pathway metabolomics predicts and provides mechanistic insight into multiple sclerosis progression. Sci Rep 2017;7. https://doi.org/10.1038/srep41473.
[76] Saraste M, Matilainen M, Rajda C, Galla Z, Sucksdorff M, Vécsei L, et al. Association between microglial activation and serum kynurenine pathway metabolites in multiple sclerosis patients. Multiple Sclerosis and Related Disorders 2022:103667. https://doi.org/10.1016/j.msard.2022.103667.
[77] Acs P, Kipp M, Norkute A, Johann S, Clarner T, Braun A, et al. 17β-estradiol and progesterone prevent cuprizone provoked demyelination of corpus callosum in male mice. Glia 2009;57:807–14. https://doi.org/10.1002/glia.20806.
[78] Veres G, Molnár M, Zádori D, Szentirmai M, Szalárdy L, Török R, et al. Central nervous system-specific alterations in the tryptophan metabolism in the 3-nitropropionic acid model of Huntington's disease. Pharmacol Biochem Behav 2015;132:115–24. https://doi.org/10.1016/j.pbb.2015.03.002.
[79] Cseh EK, Veres G, Szentirmai M, Nánási N, Szatmári I, Fülöp F, et al. HPLC method for the assessment of tryptophan metabolism utilizing separate internal standard for each detector. Anal Biochem 2019;574:7–14. https://doi.org/10.1016/j.ab.2019.03.005.
[80] Tömösi F, Kecskeméti G, Cseh EK, Szabó E, Rajda C, Kormány R, et al. A validated UHPLC-MS method for tryptophan metabolites: Application in the diagnosis of multiple sclerosis. Journal of Pharmaceutical and Biomedical Analysis 2020;185:113246. https://doi.org/10.1016/j.jpba.2020.113246.
[81] Galla Z, Rajda C, Rácz G, Grecsó N, Baráth Á, Vécsei L, et al. Simultaneous determination of 30 neurologically and metabolically important molecules: A sensitive and selective way to measure tyrosine and tryptophan pathway metabolites and other biomarkers in human serum and cerebrospinal fluid. Journal of Chromatography A 2021;1635:461775. https://doi.org/10.1016/j.chroma.2020.461775.
[82] Goldenberg MM. Multiple Sclerosis Review. P T 2012;37:175–84.
[83] Imitola J, Chitnis T, Khoury SJ. Cytokines in multiple sclerosis: from bench to bedside. Pharmacology & Therapeutics 2005;106:163–77. https://doi.org/10.1016/j.pharmthera.2004.11.007.
[84] Tan LSY, Francis HM, Lim CK. Exploring the roles of tryptophan metabolism in MS beyond neuroinflammation and neurodegeneration: A paradigm shift to neuropsychiatric symptoms. Brain Behav Immun Health 2021;12:100201. https://doi.org/10.1016/j.bbih.2021.100201.
[85] Mancuso R, Hernis A, Agostini S, Rovaris M, Caputo D, Fuchs D, et al. Indoleamine 2,3 Dioxygenase (IDO) Expression and Activity in Relapsing- Remitting Multiple Sclerosis. PLoS One 2015;10. https://doi.org/10.1371/journal.pone.0130715.
[86] Rejdak K, Bartosik-Psujek H, Dobosz B, Kocki T, Grieb P, Giovannoni G, et al. Decreased level of kynurenic acid in cerebrospinal fluid of relapsing-onset multiple sclerosis patients. Neuroscience Letters 2002;331:63–5. https://doi.org/10.1016/S0304-3940(02)00710-3.

[87] Markianos M, Koutsis G, Evangelopoulos M-E, Mandellos D, Karahalios G, Sfagos C. Relationship of CSF neurotransmitter metabolite levels to disease severity and disability in multiple sclerosis. Journal of Neurochemistry 2009;108:158–64. https://doi.org/10.1111/j.1471-4159.2008.05750.x.
[88] Joisten N, Ruas JL, Braidy N, Guillemin GJ, Zimmer P. The kynurenine pathway in chronic diseases: a compensatory mechanism or a driving force? Trends in Molecular Medicine 2021;27:946–54. https://doi.org/10.1016/j.molmed.2021.07.006.
[89] Jones SP, Franco NF, Varney B, Sundaram G, Brown DA, de Bie J, et al. Expression of the Kynurenine Pathway in Human Peripheral Blood Mononuclear Cells: Implications for Inflammatory and Neurodegenerative Disease. PLoS One 2015;10:e0131389. https://doi.org/10.1371/journal.pone.0131389.
[90] Guillemin GJ, Smith DG, Kerr SJ, Smythe GA, Kapoor V, Armati PJ, et al. Characterisation of kynurenine pathway metabolism in human astrocytes and implications in neuropathogenesis. Redox Rep 2000;5:108–11. https://doi.org/10.1179/135100000101535375.
[91] Guillemin GJ, Smythe G, Takikawa O, Brew BJ. Expression of indoleamine 2,3-dioxygenase and production of quinolinic acid by human microglia, astrocytes, and neurons. Glia 2005;49:15–23. https://doi.org/10.1002/glia.20090.
[92] Pashaei S, Yarani R, Mohammadi P, Emami Aleagha MS. The potential roles of amino acids and their major derivatives in the management of multiple sclerosis. Amino Acids 2022;54:841–58. https://doi.org/10.1007/s00726-022-03162-4.
[93] Aeinehband S, Brenner P, Ståhl S, Bhat M, Fidock MD, Khademi M, et al. Cerebrospinal fluid kynurenines in multiple sclerosis; relation to disease course and neurocognitive symptoms. Brain, Behavior, and Immunity 2016;51:47–55. https://doi.org/10.1016/j.bbi.2015.07.016.
[94] Herman S, Åkerfeldt T, Spjuth O, Burman J, Kultima K. Biochemical Differences in Cerebrospinal Fluid between Secondary Progressive and Relapsing–Remitting Multiple Sclerosis. Cells 2019;8:84. https://doi.org/10.3390/cells8020084.
[95] Komoly S. Experimental demyelination caused by primary oligodendrocyte dystrophy. Regional distribution of the lesions in the nervous system of mice [corrected]. Ideggyogy Sz 2005;58:40–3.
[96] Acs P, Selak MA, Komoly S, Kalman B. Distribution of oligodendrocyte loss and mitochondrial toxicity in the cuprizone-induced experimental demyelination model. Journal of Neuroimmunology 2013;262:128–31. https://doi.org/10.1016/j.jneuroim.2013.06.012.
[97] Titus HE, Chen Y, Podojil JR, Robinson AP, Balabanov R, Popko B, et al. Pre-clinical and Clinical Implications of "Inside-Out" vs. "Outside-In" Paradigms in Multiple Sclerosis Etiopathogenesis. Front Cell Neurosci 2020;14:599717. https://doi.org/10.3389/fncel.2020.599717.
[98] Matsushima GK, Morell P. The Neurotoxicant, Cuprizone, as a Model to Study Demyelination and Remyelination in the Central Nervous System. Brain Pathology 2001;11:107–16. https://doi.org/10.1111/j.1750-3639.2001.tb00385.x.
[99] Caprariello AV, Rogers JA, Morgan ML, Hoghooghi V, Plemel JR, Koebel A, et al. Biochemically altered myelin triggers autoimmune demyelination. Proc Natl Acad Sci U S A 2018;115:5528–33. https://doi.org/10.1073/pnas.1721115115.
[100] Sen MK, Almuslehi MSM, Gyengesi E, Myers SJ, Shortland PJ, Mahns DA, et al. Suppression of the Peripheral Immune System Limits the Central Immune Response Following Cuprizone-Feeding: Relevance to Modelling Multiple Sclerosis. Cells 2019;8:1314. https://doi.org/10.3390/cells8111314.
[101] Sen MK, Almuslehi MSM, Shortland PJ, Coorssen JR, Mahns DA. Revisiting the Pathoetiology of Multiple Sclerosis: Has the Tail Been Wagging the Mouse? Front Immunol 2020;11:572186. https://doi.org/10.3389/fimmu.2020.572186.
[102] Zhan J, Mann T, Joost S, Behrangi N, Frank M, Kipp M. The Cuprizone Model: Dos and Do Nots. Cells 2020;9. https://doi.org/10.3390/cells9040843.
[103] Goldberg J, Daniel M, van Heuvel Y, Victor M, Beyer C, Clarner T, et al. Short-Term Cuprizone Feeding Induces Selective Amino Acid Deprivation with Concomitant Activation of an Integrated

Stress Response in Oligodendrocytes. Cell Mol Neurobiol 2013;33:1087–98. https://doi.org/10.1007/s10571-013-9975-y.
[104] Tao X, Yan M, Wang L, Zhou Y, Wang Z, Xia T, et al. Homeostasis Imbalance of Microglia and Astrocytes Leads to Alteration in the Metabolites of the Kynurenine Pathway in LPS-Induced Depressive-Like Mice. Int J Mol Sci 2020;21:1460. https://doi.org/10.3390/ijms21041460.
[105] Fukui S, Schwarcz R, Rapoport SI, Takada Y, Smith QR. Blood–Brain Barrier Transport of Kynurenines: Implications for Brain Synthesis and Metabolism. Journal of Neurochemistry 1991;56:2007–17. https://doi.org/10.1111/j.1471-4159.1991.tb03460.x.
[106] Kita T, Morrison PF, Heyes MP, Markey SP. Effects of systemic and central nervous system localized inflammation on the contributions of metabolic precursors to the L-kynurenine and quinolinic acid pools in brain. J Neurochem 2002;82:258–68. https://doi.org/10.1046/j.1471-4159.2002.00955.x.
[107] Capucciati A, Galliano M, Bubacco L, Zecca L, Casella L, Monzani E, et al. Neuronal Proteins as Targets of 3-Hydroxykynurenine: Implications in Neurodegenerative Diseases. ACS Chem Neurosci 2019;10:3731–9. https://doi.org/10.1021/acschemneuro.9b00265.
[108] Lovelace MD, Varney B, Sundaram G, Lennon MJ, Lim CK, Jacobs K, et al. Recent evidence for an expanded role of the kynurenine pathway of tryptophan metabolism in neurological diseases. Neuropharmacology 2017;112:373–88. https://doi.org/10.1016/j.neuropharm.2016.03.024.
[109] Zinger A, Barcia C, Herrero MT, Guillemin GJ. The involvement of neuroinflammation and kynurenine pathway in Parkinson's disease. Parkinsons Dis 2011;2011:716859. https://doi.org/10.4061/2011/716859.
[110] Schwarcz R, Bruno JP, Muchowski PJ, Wu H-Q. KYNURENINES IN THE MAMMALIAN BRAIN: WHEN PHYSIOLOGY MEETS PATHOLOGY. Nat Rev Neurosci 2012;13:465–77. https://doi.org/10.1038/nrn3257.
[111] Oxenkrug G, van der Hart M, Roeser J, Summergrad P. Anthranilic Acid: A Potential Biomarker and Treatment Target for Schizophrenia. Ann Psychiatry Ment Health 2016;4.
[112] Cathomas F, Guetter K, Seifritz E, Klaus F, Kaiser S. Quinolinic acid is associated with cognitive deficits in schizophrenia but not major depressive disorder. Sci Rep 2021;11:9992. https://doi.org/10.1038/s41598-021-89335-9.
[113] Bloomfield PS, Selvaraj S, Veronese M, Rizzo G, Bertoldo A, Owen DR, et al. Microglial Activity in People at Ultra High Risk of Psychosis and in Schizophrenia: An [(11)C]PBR28 PET Brain Imaging Study. Am J Psychiatry 2016;173:44–52. https://doi.org/10.1176/appi.ajp.2015.14101358.
[114] Brisch R, Wojtylak S, Saniotis A, Steiner J, Gos T, Kumaratilake J, et al. The role of microglia in neuropsychiatric disorders and suicide. European Archives of Psychiatry and Clinical Neuroscience 2022;272:929–45. https://doi.org/10.1007/s00406-021-01334-z.
[115] Cakmak JD, Liu L, Poirier SE, Schaefer B, Poolacherla R, Burhan AM, et al. The functional and structural associations of aberrant microglial activity in major depressive disorder. J Psychiatry Neurosci 2022;47:E197–208. https://doi.org/10.1503/jpn.210124.
[116] Okuda S, Nishiyama N, Saito H, Katsuki H. 3-Hydroxykynurenine, an Endogenous Oxidative Stress Generator, Causes Neuronal Cell Death with Apoptotic Features and Region Selectivity. Journal of Neurochemistry 1998;70:299–307. https://doi.org/10.1046/j.1471-4159.1998.70010299.x.
[117] Chobot V, Hadacek F, Weckwerth W, Kubicova L. Iron chelation and redox chemistry of anthranilic acid and 3-hydroxyanthranilic acid: A comparison of two structurally related kynurenine pathway metabolites to obtain improved insights into their potential role in neurological disease development. J Organomet Chem 2015;782:103–10. https://doi.org/10.1016/j.jorganchem.2015.01.005.
[118] González Esquivel D, Ramírez-Ortega D, Pineda B, Castro N, Ríos C, Pérez de la Cruz V. Kynurenine pathway metabolites and enzymes involved in redox reactions. Neuropharmacology 2017;112:331–45. https://doi.org/10.1016/j.neuropharm.2016.03.013.

[119] Lima VLA, Dias F, Nunes RD, Pereira LO, Santos TSR, Chiarini LB, et al. The Antioxidant Role of Xanthurenic Acid in the Aedes aegypti Midgut during Digestion of a Blood Meal. PLoS One 2012;7:e38349. https://doi.org/10.1371/journal.pone.0038349.
[120] Murakami K, Ito M, Yoshino M. Xanthurenic acid inhibits metal ion-induced lipid peroxidation and protects NADP-isocitrate dehydrogenase from oxidative inactivation. J Nutr Sci Vitaminol (Tokyo) 2001;47:306–10. https://doi.org/10.3177/jnsv.47.306.
[121] Pérez-González A, Alvarez-Idaboy JR, Galano A. Free-radical scavenging by tryptophan and its metabolites through electron transfer based processes. J Mol Model 2015;21:213. https://doi.org/10.1007/s00894-015-2758-2.
[122] Baran H, Staniek K, Kepplinger B, Stur J, Draxler M, Nohl H. Kynurenines and the respiratory parameters on rat heart mitochondria. Life Sciences 2003;72:1103–15. https://doi.org/10.1016/S0024-3205(02)02365-2.
[123] Badawy AA-B. Hypothesis kynurenic and quinolinic acids: The main players of the kynurenine pathway and opponents in inflammatory disease. Medical Hypotheses 2018;118:129–38. https://doi.org/10.1016/j.mehy.2018.06.021.
[124] Negrotto L, Correale J. Amino Acid Catabolism in Multiple Sclerosis Affects Immune Homeostasis. The Journal of Immunology 2017;198:1900–9. https://doi.org/10.4049/jimmunol.1601139.
[125] El-Sewedy SM, Abdel-Tawab GA, El-Zoghby SM, Zeitoun R, Mostafa MH, Shalaby ShM. Studies with tryptophan metabolites in vitro. effect of zinc, manganese, copper and cobalt ions on kynurenine hydrolase and kynurenine aminotransferase in normal mouse liver. Biochemical Pharmacology 1974;23:2557–65. https://doi.org/10.1016/0006-2952(74)90178-6.
[126] Ljutakova SG, Russanov EM. Differences in the in vivo effects of cuprizone on superoxide dismutase activity in rat liver cytosol and mitochondrial intermembrane space. Acta Physiol Pharmacol Bulg 1985;11:56–61.
[127] Zhang Y, Xu H, Jiang W, Xiao L, Yan B, He J, et al. Quetiapine alleviates the cuprizone-induced white matter pathology in the brain of C57BL/6 mouse. Schizophrenia Research 2008;106:182–91. https://doi.org/10.1016/j.schres.2008.09.013.
[128] Zhang X, McIntire WS. Cloning and sequencing of a copper-containing, topa quinone-containing monoamine oxidase from human placenta. Gene 1996;179:279–86. https://doi.org/10.1016/S0378-1119(96)00387-3.
[129] Fridovich I. Superoxide Dismutases. Annual Review of Biochemistry 1975;44:147–59. https://doi.org/10.1146/annurev.bi.44.070175.001051.
[130] Horn D, Barrientos A. Mitochondrial Copper Metabolism and Delivery to Cytochrome c Oxidase. IUBMB Life 2008;60:421–9. https://doi.org/10.1002/iub.50.
[131] Blackburn NJ, Mason HS, Knowles PF. Dopamine-β-hydroxylase: Evidence for binuclear copper sites. Biochemical and Biophysical Research Communications 1980;95:1275–81. https://doi.org/10.1016/0006-291X(80)91611-3.
[132] Takahashi Y, Kako K, Kashiwabara S, Takehara A, Inada Y, Arai H, et al. Mammalian Copper Chaperone Cox17p Has an Essential Role in Activation of Cytochrome c Oxidase and Embryonic Development. Mol Cell Biol 2002;22:7614–21. https://doi.org/10.1128/MCB.22.21.7614-7621.2002.
[133] Herring NR, Konradi C. MYELIN, COPPER, AND THE CUPRIZONE MODEL OF SCHIZOPHRENIA. Front Biosci (Schol Ed) 2011;3:23–40.
[134] Kesterson JW, Carlton WW. Cuprizone toxicosis in mice—Attempts to antidote the toxicity. Toxicology and Applied Pharmacology 1972;22:6–13. https://doi.org/10.1016/0041-008X(72)90220-7.
[135] Biancotti JC, Kumar S, de Vellis J. Activation of inflammatory response by a combination of growth factors in cuprizone-induced demyelinated brain leads to myelin repair. Neurochem Res 2008;33:2615–28. https://doi.org/10.1007/s11064-008-9792-8.

[136] Venturini G. Enzymic Activities and Sodium, Potassium and Copper Concentrations in Mouse Brain and Liver After Cuprizone Treatment in Vivo. Journal of Neurochemistry 1973;21:1147–51. https://doi.org/10.1111/j.1471-4159.1973.tb07569.x.
[137] Sadok I, Gamian A, Staniszewska MM. Chromatographic analysis of tryptophan metabolites. J Sep Sci 2017;40:3020–45. https://doi.org/10.1002/jssc.201700184.